



NBS REPORT

7267

Quarterly Report

for

March 1, 1962 to June 1, 1962

on

ELASTOMERIC SEALS AND MATERIALS

AT

CRYOGENIC TEMPERATURES

by

R. F. Robbins, Y. Ohori, P. R. Ludtke and D. H. Weitzel



PROPERTY OF
SOUTHWEST RESEARCH INSTITUTE LIBRARY
SAN ANTONIO, TEXAS

U. S. DEPARTMENT OF COMMERCE
NATIONAL BUREAU OF STANDARDS
BOULDER LABORATORIES
Boulder, Colorado

THE NATIONAL BUREAU OF STANDARDS

Functions and Activities

The functions of the National Bureau of Standards are set forth in the Act of Congress, March 3, 1901, as amended by Congress in Public Law 619, 1950. These include the development and maintenance of the national standards of measurement and the provision of means and methods for making measurements consistent with these standards; the determination of physical constants and properties of materials; the development of methods and instruments for testing materials, devices, and structures; advisory services to government agencies on scientific and technical problems; invention and development of devices to serve special needs of the Government; and the development of standard practices, codes, and specifications. The work includes basic and applied research, development, engineering, instrumentation, testing, evaluation, calibration services, and various consultation and information services. Research projects are also performed for other government agencies when the work relates to and supplements the basic program of the Bureau or when the Bureau's unique competence is required. The scope of activities is suggested by the listing of divisions and sections on the inside of the back cover.

Publications

The results of the Bureau's research are published either in the Bureau's own series of publications or in the journals of professional and scientific societies. The Bureau itself publishes three periodicals available from the Government Printing Office: The Journal of Research, published in four separate sections, presents complete scientific and technical papers; the Technical News Bulletin presents summary and preliminary reports on work in progress; and Basic Radio Propagation Predictions provides data for determining the best frequencies to use for radio communications throughout the world. There are also five series of non-periodical publications: Monographs, Applied Mathematics Series, Handbooks, Miscellaneous Publications, and Technical Notes.

A complete listing of the Bureau's publications can be found in National Bureau of Standards Circular 460, Publications of the National Bureau of Standards, 1901 to June 1947 (\$1.25), and the Supplement to National Bureau of Standards Circular 460, July 1947 to June 1957 (\$1.50), and Miscellaneous Publication 240, July 1957 to June 1960 (Includes Titles of Papers Published in Outside Journals 1950 to 1959) (\$2.25); available from the Superintendent of Documents, Government Printing Office, Washington 25, D. C.

NATIONAL BUREAU OF STANDARDS REPORT

NBS PROJECT

81429

June 25, 1962

NBS REPORT

7267

ASD 33(616) 61-04

Quarterly Report

for

March 1, 1962, to June 1, 1962

on

ELASTOMERIC SEALS AND MATERIALS

AT

CRYOGENIC TEMPERATURES

by

R. F. Robbins, Y. Ohori, P. R. Ludtke, and D. H. Weitzel



U. S. DEPARTMENT OF COMMERCE
NATIONAL BUREAU OF STANDARDS
BOULDER LABORATORIES
Boulder, Colorado

IMPORTANT NOTICE

NATIONAL BUREAU OF STANDARDS REPORTS are usually
intended for use within the Government
and are not to be distributed outside the
Government without the approval of the
Director of the National Institute of
Standards and Technology (NIST) on
October 9, 2015.

Approved for public release by the
Director of the National Institute of
Standards and Technology (NIST) on
October 9, 2015.

Printing docu-
published it
l, reproduc-
unless per-
Washington
Report has
se.

FOREWORD

This report was prepared by the National Bureau of Standards under USAF Contract No. 33(616)-61-04. This contract was initiated under Project No. 7340, "Nonmetallic and Composite Materials", Task No. 73405. "Elastomeric and Compliant Materials". The work was administered under the direction of Directorate of Materials and Processes, Deputy for Technology, Aeronautical Systems Division, with Mr. Roger Headrick acting as Project Engineer.

Program Status

The fundamental studies concerning force evaluation of compressed O-rings and thermal expansion have continued during the reporting period. All of the force decay data taken to date will be reported herein, together with sealability information recorded simultaneously. Thermal expansion curves for Group II will be reported to add to those previously presented.

Differential Thermal Analysis tests have stopped temporarily, due to the development and preliminary testing of an apparatus designed to study the dependence of the glassy state transition on volume compression. The latter will be discussed in this report. An apparatus designed to measure resilience using an automatic, free-fall scheme is nearing completion, and will be described in the next quarterly report.

All of the above mentioned tests are performed over the temperature range 300°K to 76°K.

1.0 Force Evaluation Experiment

(P. R. L.)

1.1 Introduction

The purpose of this experiment is to measure the force on an O-ring while it is compressed and held at constant thickness during cooldown from room temperature to 76°K. The O-ring functions as a seal during the experiment, and the force and temperature at which a leak begins is noted. In addition, the force-temperature curve is continuously recorded so that not only the end points but the shapes of the curves for various elastomers can be compared.

The test apparatus is shown in Figure 1. The plates and bolts are oversized to minimize flexing or stretching, which would place a spring load on the O-ring. Spring loading is desirable in the practical seal application, but more meaningful comparisons of the various elastomers can be obtained in this experiment if spring loading is minimized or eliminated. The stressed parts of the jig are made of invar. This includes force washer sleeves, top plate, studs, pillars, and compression disc. The pillars are placed adjacent to the studs between the base and top plate to maintain a constant separation

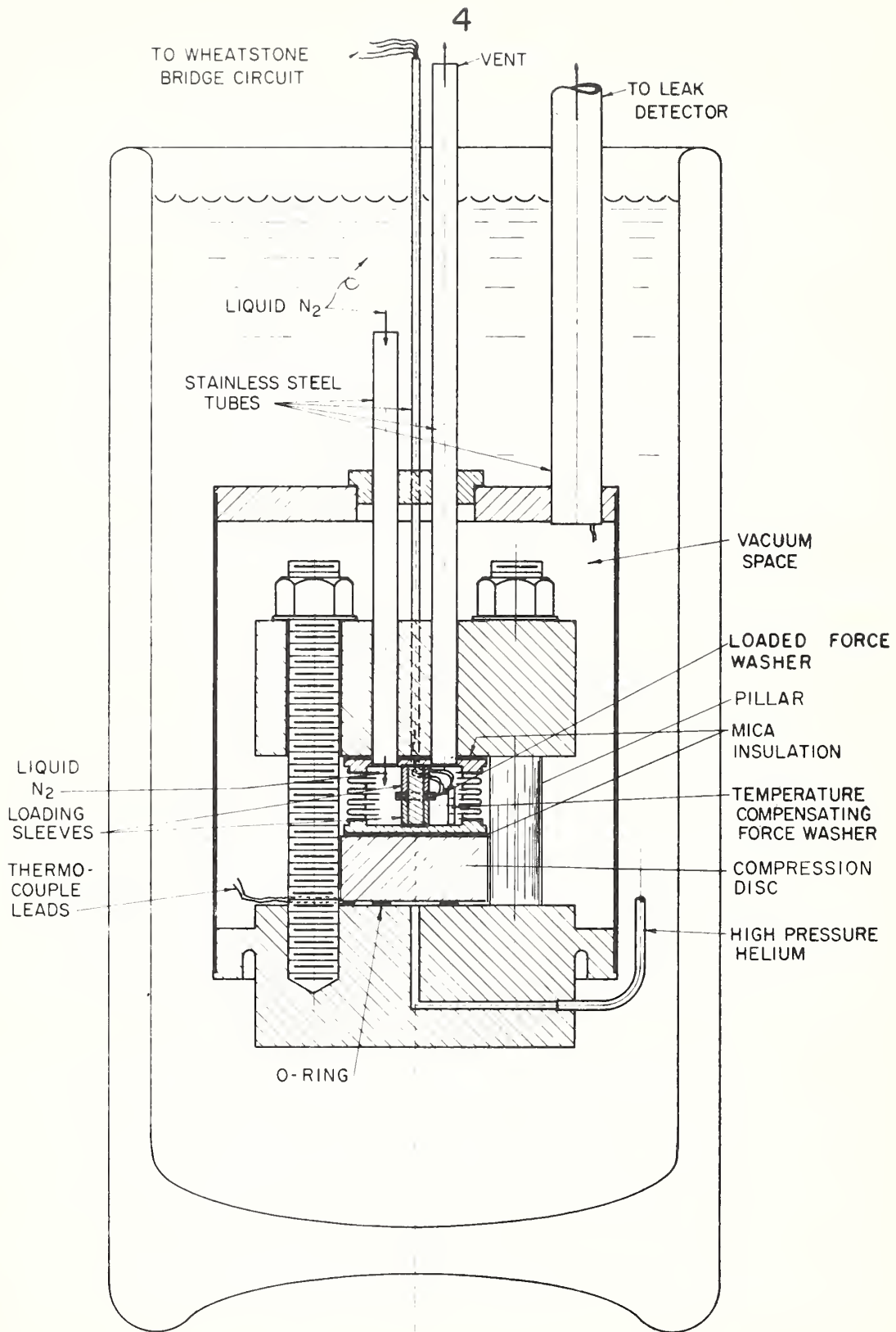


Figure 1. Force - Temperature Test Apparatus

between these surfaces and keep them accurately parallel at all times. This insures uniform compression of the O-ring and maintains constant thickness during cooldown.

The bellows assembly contains three washer type strain gages. Liquid nitrogen is circulated through the bellows to maintain the force washers at a constant temperature and to slowly cool the apparatus. A thermocouple placed beside the O-ring provides a record of O-ring temperature. The force washers and three external fixed resistors constitute a bridge circuit which provides a signal proportional to the force on the O-ring. The force and temperature signals are continuously recorded during a cooldown cycle.

1.2 Procedure

The 0.140 inch thick x 1 inch I. D. O-ring is given an arbitrary initial force of approximately 14,000 pounds. The force is adjusted by varying the number of mica shims between the compression disc and bellows. After the O-ring is compressed to the thickness required for 14,000 pounds of force, the outer cover is soldered to the base of the test jig with Rose's fusible metal. This metal has a melting point of 96°C compared to 185°C for the 50-50 tin based solder previously used. This greatly decreases the amount of heat required for soldering and the heat conducted to the compressed O-ring. Soldering still warms the O-ring slightly and accelerates the relaxation of the elastomer.

After the test jig cools to room temperature the force is measured again to determine the amount of force lost during this initial relaxation period. This is the force at the start of the first cooldown cycle. The O-ring is then cooled to 76°K. During the first cooldown cycle the helium pressure inside the compressed O-ring is 100 psig. If the O-ring does not leak during the first cooldown cycle, the helium pressure is increased to 500 psig during the second cooldown cycle. If no leak occurs during the second cooldown cycle the helium pressure is increased to 1,000 psig for the third and last cooldown cycle. If a leak occurs, the helium pressure is not increased for the following cooldown cycles.

The percent of error in the force measurement during cooldown is comparatively high. If the apparatus is assembled with zero initial force on the O-ring, the force will vary from 600 to 1500 pounds from the zero setting. Consequently, when the force at start of cooldown

is small, the percent of error is high. If the force at start of cool-down is less than 3,000 pounds, the force measured during cooldown is considered too much in error. Straight dashed lines appear on the temperature-force figures for these cooldown cycles. All force measurements at ambient temperatures should be reasonably accurate.

1.3 Results and Discussion

Groups I, II, and IV of the elastomer samples provided have been tested to date. Meaningful results have been obtained and will be discussed in detail.

The compounds in group I all have the characteristic of losing most of the initial force during the initial relaxation period. This is the period in which the outer cover is soldered to the base of the jig and the entire jig is then allowed to cool back to room temperature. This force loss was so drastic for the group I polymers that separate measurements of force decay were taken at room temperature. These force measurements were taken with no cover on the test apparatus, and no heat from soldering present. The results are shown in table I. The polymers in this group averaged 42% loss of force after being compressed for one hour. These compounds will sustain a high initial force but cannot maintain this force. The O-rings tend to flow or relax and lose most of the initial force before cooldown.

The results of tests on "Viton" A(I-8D), * "Viton" A-HV (I-12B), and "Viton" B (I-12A) were similar. These are shown in table 2 and figures 2, 3 and 4. These elastomer samples lost 79-90 percent of the initial force before being cooled down and the O-rings leaked at relatively high temperatures ($\approx 230^{\circ}\text{K}$). This is 10 degrees below T_g for the "Vitons". However, the leak rate was small and there was no material failure.

In previous tests the vinylidene fluoride-perfluoropropylene polymers have maintained a seal at cryogenic temperatures where spring loading, volume compression (tongue and groove) or some type of radial confinement (retaining sleeve) was inherent to the jig. However, in the present tests the O-ring is compressed between two rigid, parallel plates. There is negligible spring loading, no radial confinement other than radial friction, and probably not much volume compression. The resulting seal performance of these polymers was relatively poor.

*All trademarks are noted by quotation marks, and are credited in the table of compounding recipes given in the appendix.

Polymer	A. S. D. Compound Number	Initial Force (lbs.)	Force After One Hour (lbs.)	Percent of Initial Force Lost in One Hour
"Viton" A (Du Pont)	I- 8D	14,700	8600	42%
"Viton" A-HV (Du Pont)	I-12B	17,800	11,200	37%
"Viton" B (Du Pont)	I-12A	14,600	7400	50%
"Kel F" 5500 (Minnesota Mining & Mfg. Co.)	I-12D	17,600	10,500	40%
"Kel F" 3700 (Minnesota Mining & Mfg. Co.)	I-12E	14,700	6700	55%
"Fluorel" (Minnesota Mining & Mfg. Co.)	I-12C	14,000	9700	30%

TABLE 1

Force Decay at Room Temperature

Polymer	A. S. D. Compound Number	Shore A. Hardness	Initial Force (lbs.)	Percent Force Lost During Initial Relaxation	Compressed O-ring Thickness	Percent Compression	Compression Set	Material Failure	Force at Start of Cooldown			Leak Occurred				L. R. at 76°K x 10 ⁶ (atm cm ³ /sec)
									#1	#2	#3	Temp. (°K)	Force (lbs.)	He. Pres. (p. s. i. g.)	Off Scale Time***	
Group #I																
"Viton" A (Du Pont)	I-8D	80	14,000	80%	.037"	74%	46%	None	2800	<500	<500	209 250 252	1500 <500 <500	100 100 100	26 min. 30 min. 38 min.	
"Viton" A-HV (Du Pont)	I-12B	80	14,000	79%	.033"	76%	71%	None	3000	<500	<500	233 250 256	1800 <500 <500	100 100 100	32 min. 36 min. 37 min.	
"Viton" B (Du Pont)	I-12A	75	14,600	90%	.028"	80%	56%	None	1500	700	700	233 238 240	<500 <500 <500	100 100 100	32 min. 33 min. 37 min.	
"Kel F" 5500 (Minnesota Mining & Mfg.)	I-12D	80	13,800	93%	.020"	86%	88%	Severe	1000	<500	<500	241 241 244	<500 <500 <500	100 100 100	22 min. 17 min. 15 min.	
"Kel Fu 3700 (Minnesota Mining & Mfg.)	I-12E	75	14,700	80%	.013"	93%	83%	Severe	3000	<500	<500	233 236 237	<500 <500 <500	100 100 100	1 min. 1 sec. 1 sec.	
"Fluorel" (Minnesota Mining & Mfg.)	I-12C	80	14,000	67%	.033"	76%	52%	None	4600	2300	2200	232 235 236	3000 ---- ----	100 100 100	6 min. 6 min. 4 min.	
Group #II																
"Synpol" 1013 (U. S. Chem. Co.)	II-21E	70	12,600	63%	.027"	81%	34%	None	4600	4100	3200	104 147 146	1700 800 ----	100 500 500	11 min. 5 min.	5
"Paracril" 18/80 (Naugatuck Chem. Division)	II-21A	75	14,000	31%	.024"	83%	39%	None	9600	8100	7400	185 192 195	5500 5000 4800	100 100 100	12 min. 9 min. 13 min.	
"Hycar" 1002 (B. F. Goodrich Chem. Company)	II-21B	75	14,200	27%	.034"	76%	32%	None	10,300	7500	6700	104 125 104	5700 5000 4200	100 100 500	18 min.	165 260
"Paracril" D (Naugatuck Chem. Division)	II-21C	85	14,300	53%	.034"	76%	47%	None	6700	2000	2000	241 274 277	4400 ---- ----	100 100 100	36 min. 40 min. 42 min.	
"Synpol" 1000 (U. S. Chem. Co.)	II-21D	65	13,400	30%	.026"	81%	30%	None	10,000	6100	5800	200 204 202	7200 3100 2900	100 100 100	15 min. 23 min. 22 min.	
Group #IV																
EPR-40	IV-29C	60	14,000	21%	.018"	87%	33%	None	11,000	9000	8800	196 208 ---	5800 5300 ----	100 100 ---	1 min. 11 min. -----	
Cis-4 Polybutadiene	IV-29B	70	14,000	19%	.032"	77%	23%	None	11,500	8000	7500	-----	-----	-----	No Leak Occurred	
Natural Rubber	IV-8A	65	14,200	17%	.023"	84%	64%	None	11,800	9200	9200	123 154 169 167	400 7500 6500 6300	1000 100 100 100	1 sec. 26 min. 21 min. 16 min.	
Polyisoprene	IV-29A	70	14,000	18%	.026"	81%	70%	None	10,000	7200	7200	88 122 122	4100 2300 2600	100 500 500	1 sec. 1 sec.	8
"Neoprene" (Du Pont)	IV-8B	75	13,500	48%	.030"	79%	85%	None	7100	5100	4800	179 200 207	2700 2500 2300	100 100 100	13 min. 18 min. 19 min.	
Natural Rubber *	IV-8A	65	18,000	27%	.024"	83%	58%	None	13,000	12,000	12,000	-----	-----	-----	No Leak Occurred	
												76°K***	7400	1250	1 sec.	

* 18,000# initial force instead of usual 14,000#.

** A leak occurred when the test jig was removed from the liquid nitrogen bath and set down on the concrete floor.

*** Time required for leak rate to increase from zero to 3×10^{-4} atm cc/sec.

TABLE 2 - FORCE EVALUATION TEST DATA

B-34315

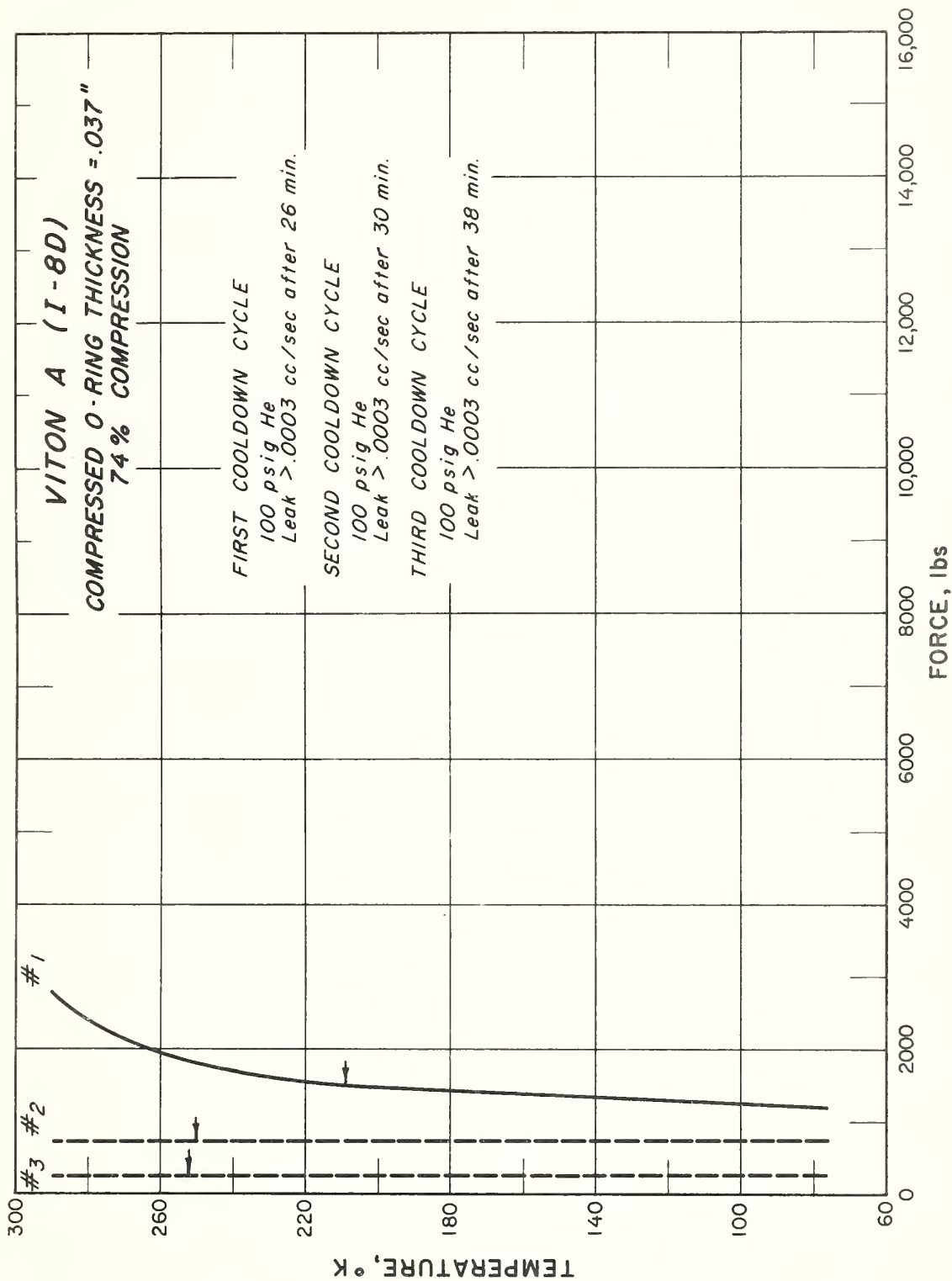


Figure 2. Force-Temperature Curve, "Viton" A

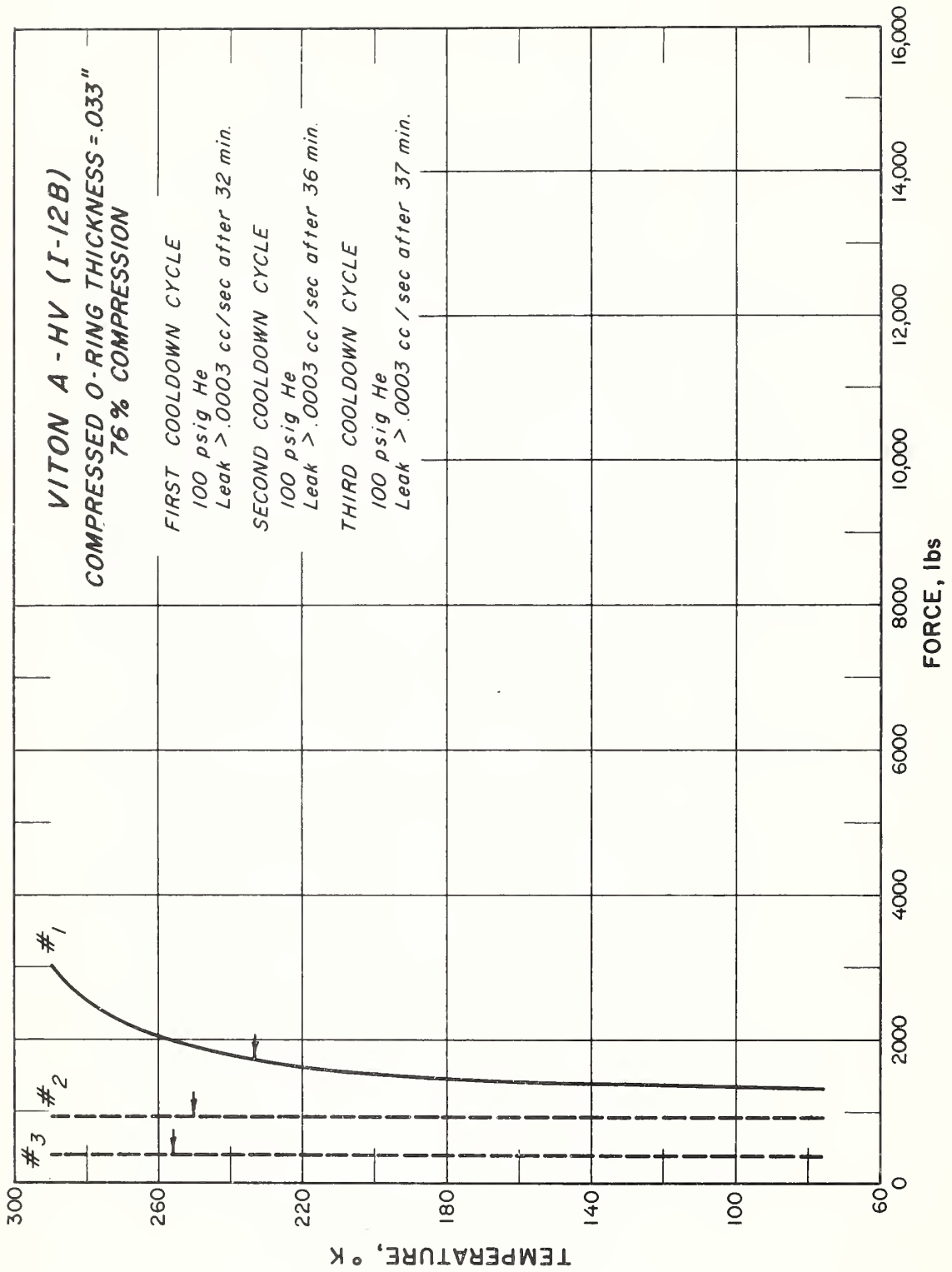


Figure 3. Force-Temperature Curve, "Viton" A-HV

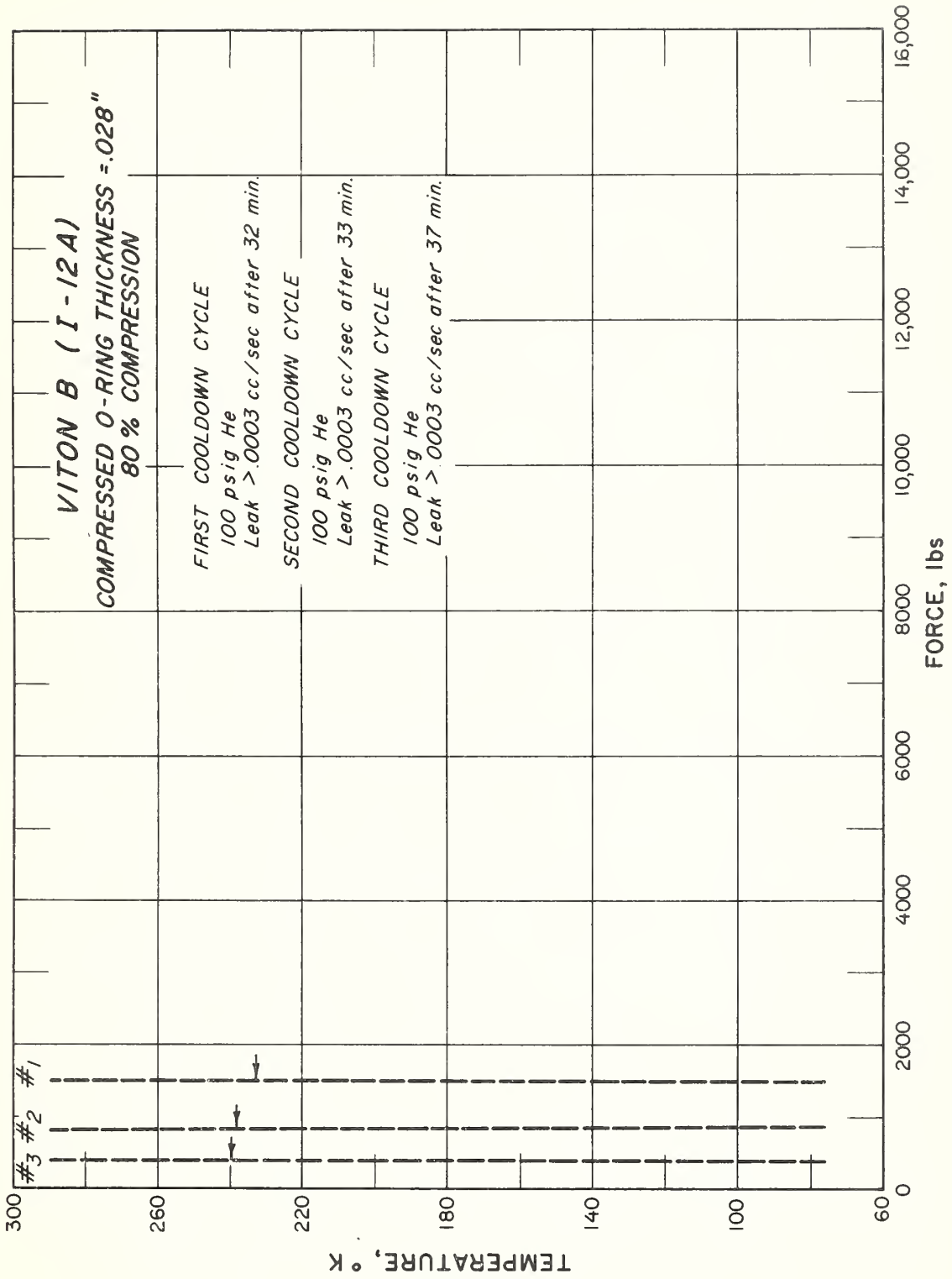


Figure 4. Force-Temperature Curve, "Viton" B

"Kel F"-3700 (I-12E) and "Kel F"-5500 (I-12A), figures 5 and 6, performed similar to the "Viton" compounds. There was a higher percentage of initial force lost (80-93%), probably because of severe material failure. The "Kel F"-3700 O-ring held together better than the "Kel F"-5500 O-ring. The latter was completely shredded and it is surprising a seal was maintained at room temperature. Neither of these elastomers is suited for seal application under these high forces. "Fluorel" (I-12C), figure 7, had the least initial force loss of this group (67%) and maintained the remaining force slightly better than the other compounds. There was no material failure.

The compounds in group I all leaked at approximately the same temperature (230°K) and none of the O-rings held 100 psig helium at 76°K. The immediate force decay of the compounds in this group is probably due to the less rigid nitrogen cross-linking bonds. However, there was no visible material failure of the vinylidene fluoride-perfluoropropylene polymers at 14,000 pounds force.

There was no characteristic pattern of behavior for the elastomer samples of group II. "Synpol" 1000 (II-21D), figure 12, maintained a considerable amount of force but the leak temperature was relatively high (200°K). "Synpol" 1013 (II-21E), figure 8, maintained less force than "Synpol" 1000 but the leak temperature was much lower. The seal began leaking at 104°K. At 76°K the leak rate was constant at 5×10^{-6} atm cc/sec. The helium pressure inside the O-ring was increased to 500 psig for the second cooldown and the O-ring began leaking at 147°K. After eleven more minutes of cooling the leak rate was greater than 0.0003 atm cc/sec., the maximum reading on the leak detector. Comparing these two butadiene-styrene polymers, one can conclude that "Synpol" 1000 maintains the initial force better but "Synpol" 1013 leaks at a much lower temperature and should give better performance in a seal application.

"Paracril" D (II-21C), figure 11, lost 53% of the initial force before cooldown and maintained only 2,000 pounds of force after the first cooldown. The leak temperatures were high ($\approx 260^\circ\text{K}$). "Paracril" 80-18 (II-21A), figure 9, performed much better. Only 31% of the initial force was lost and the O-ring maintained 8100 pounds of force after the first cooldown. The leak temperatures were approximately 190°K. "Hycar" 1002 (II-21B), figure 10,

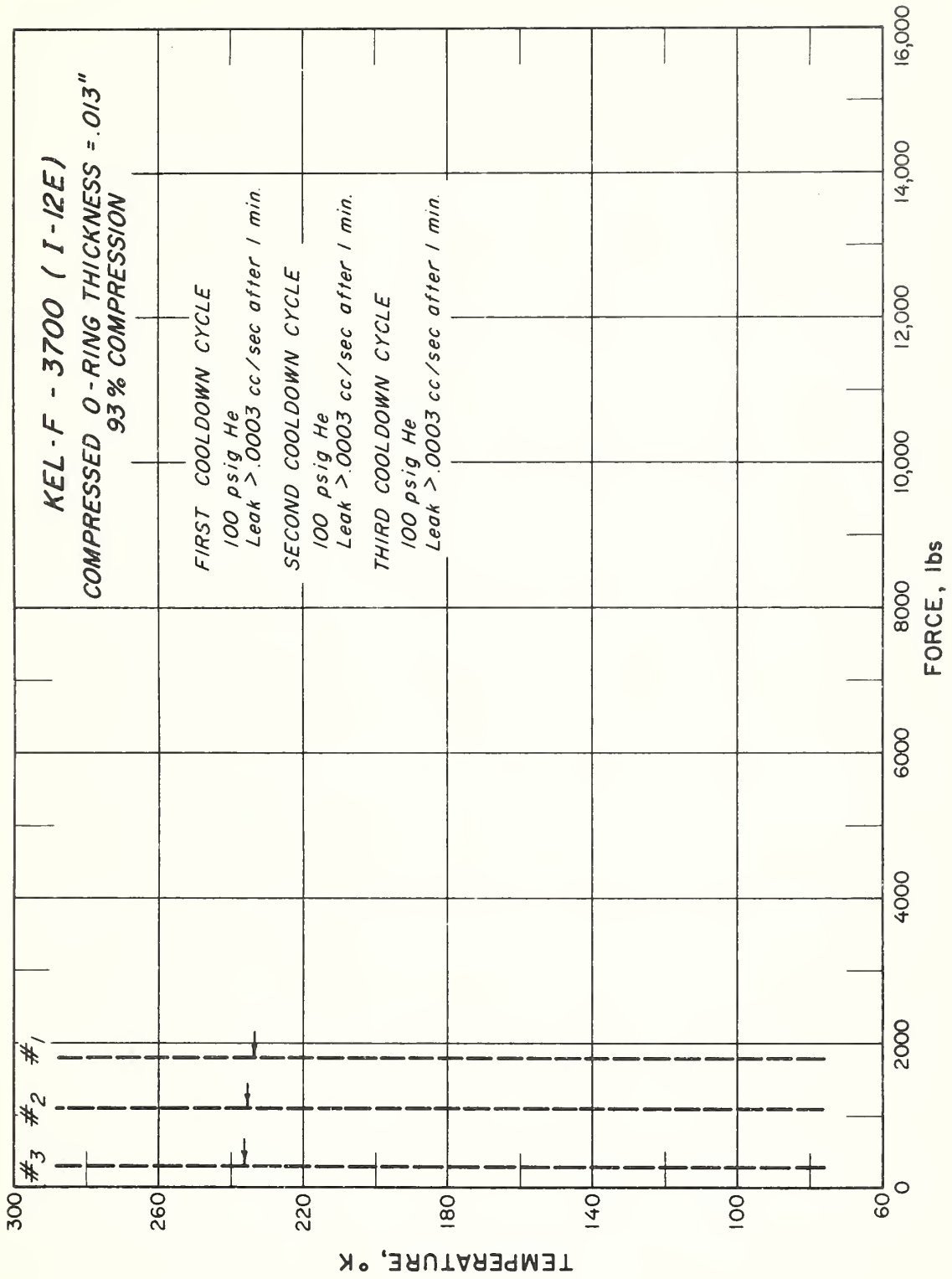


Figure 5. Force-Temperature Curve, "Kel F" 3700

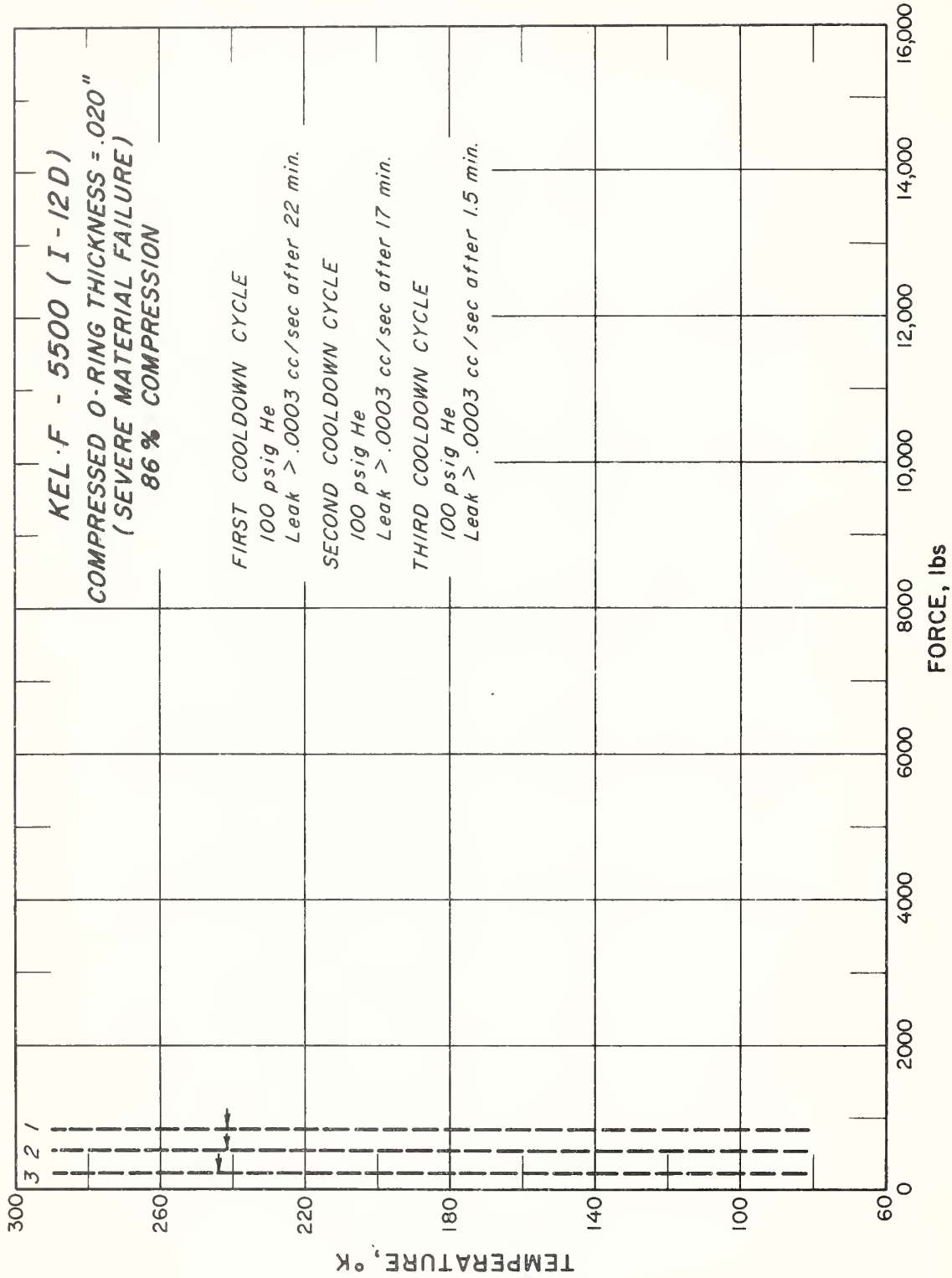


Figure 6. Force-Temperature Curve, "Kel F" 5500

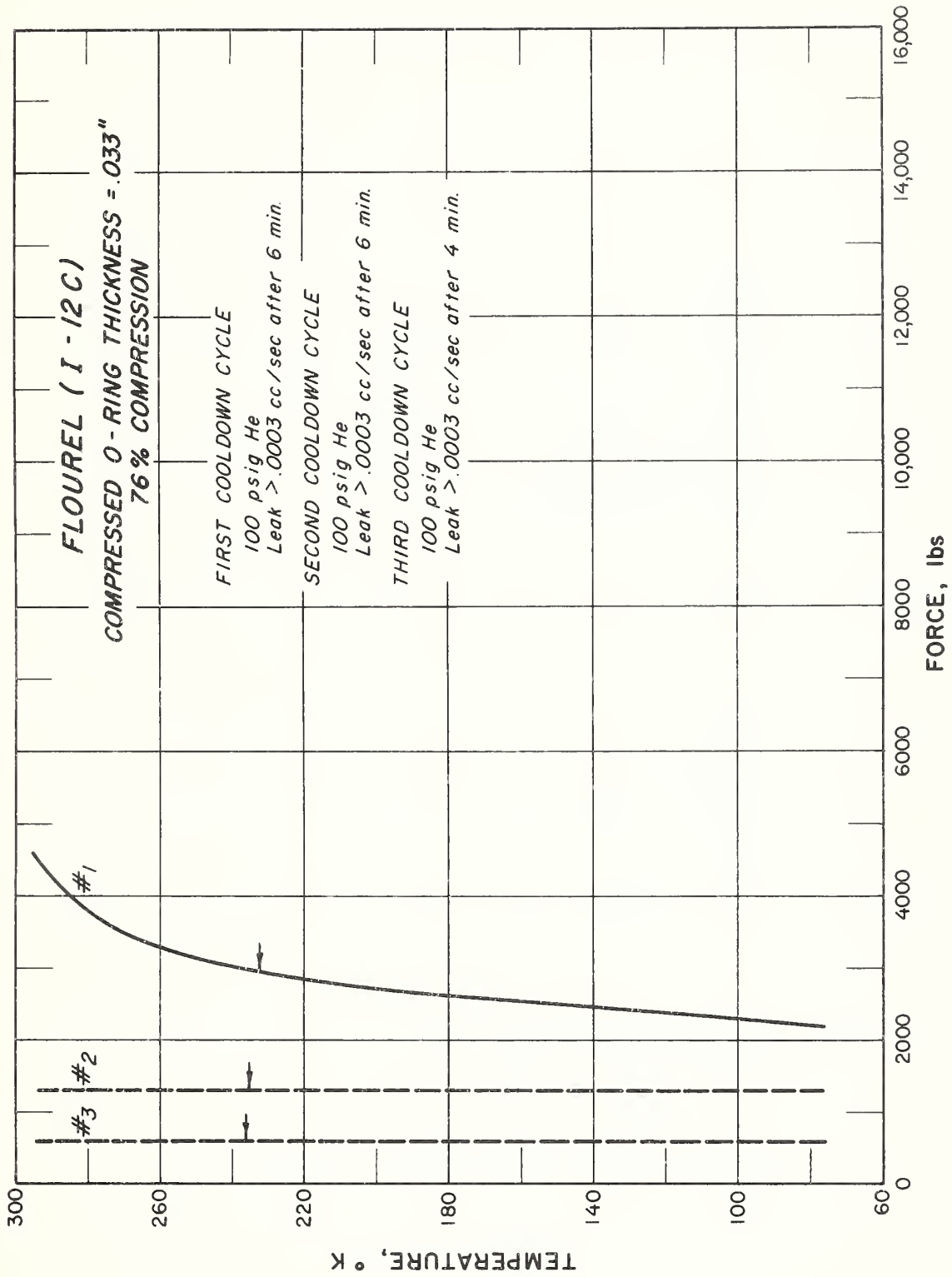


Figure 7. Force-Temperature Curve, "Fluorel"

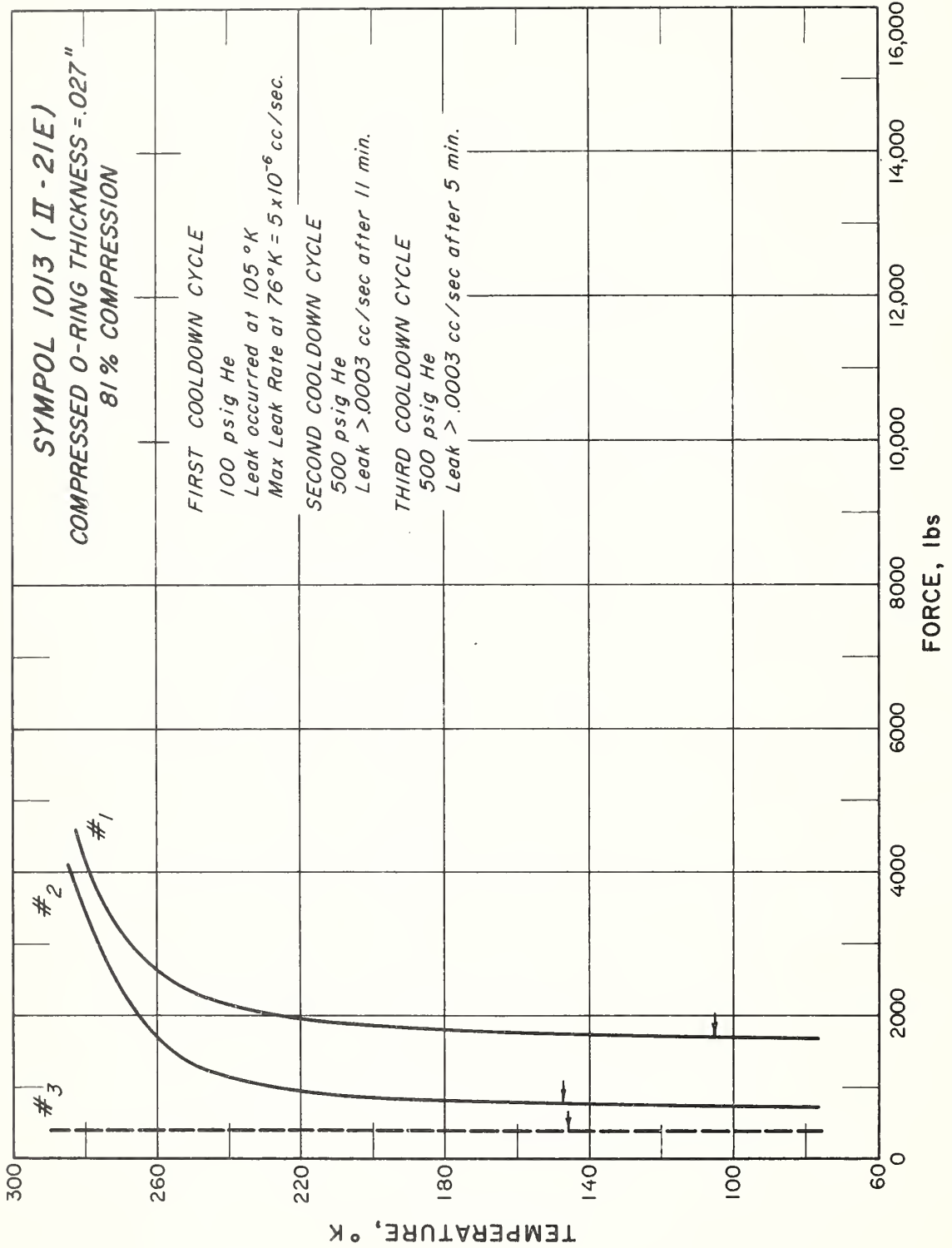


Figure 8. Force-Temperature Curve, "Sympol" 1013

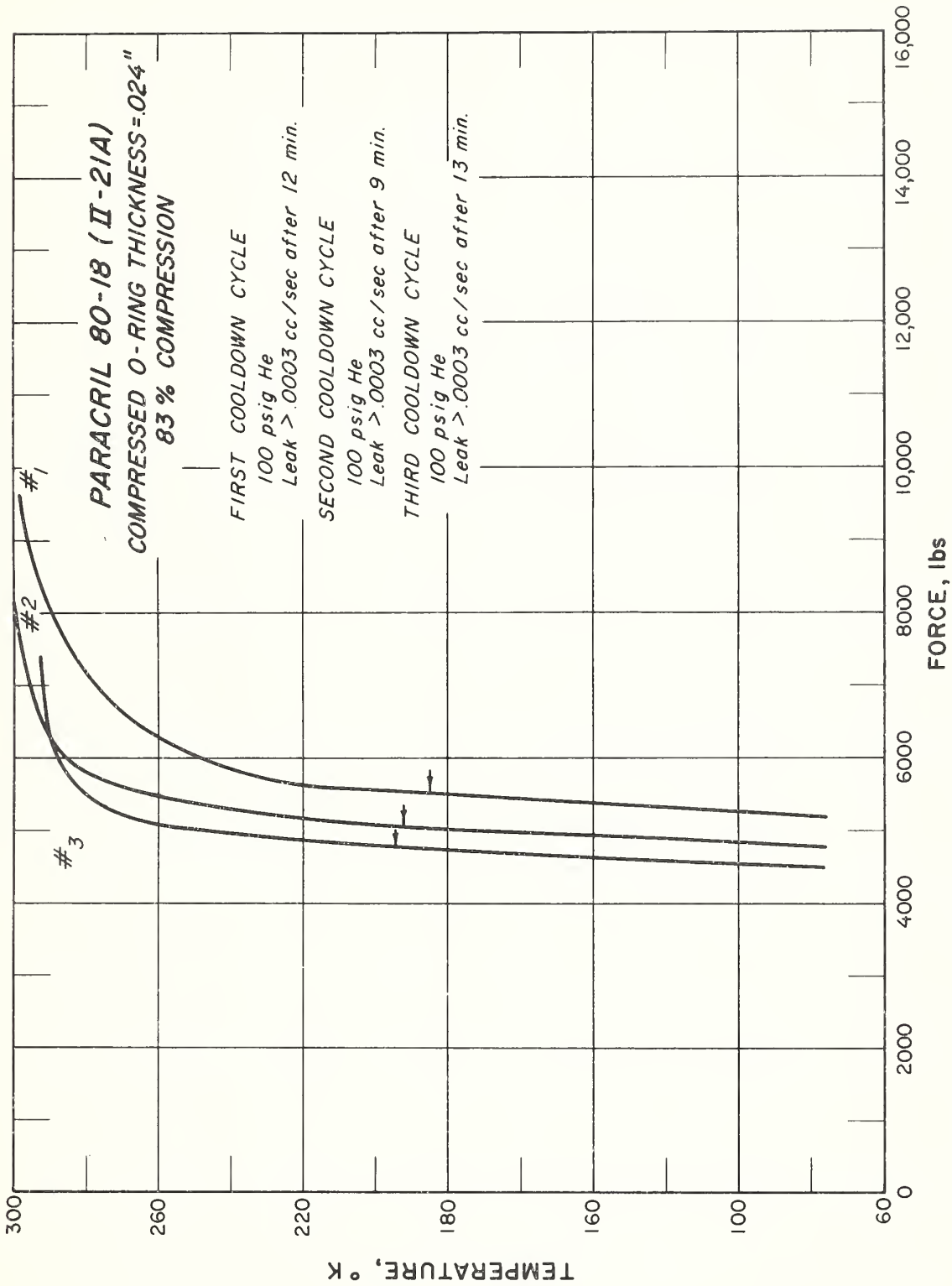


Figure 9. Force-Temperature Curve, "Paracril" 18/80

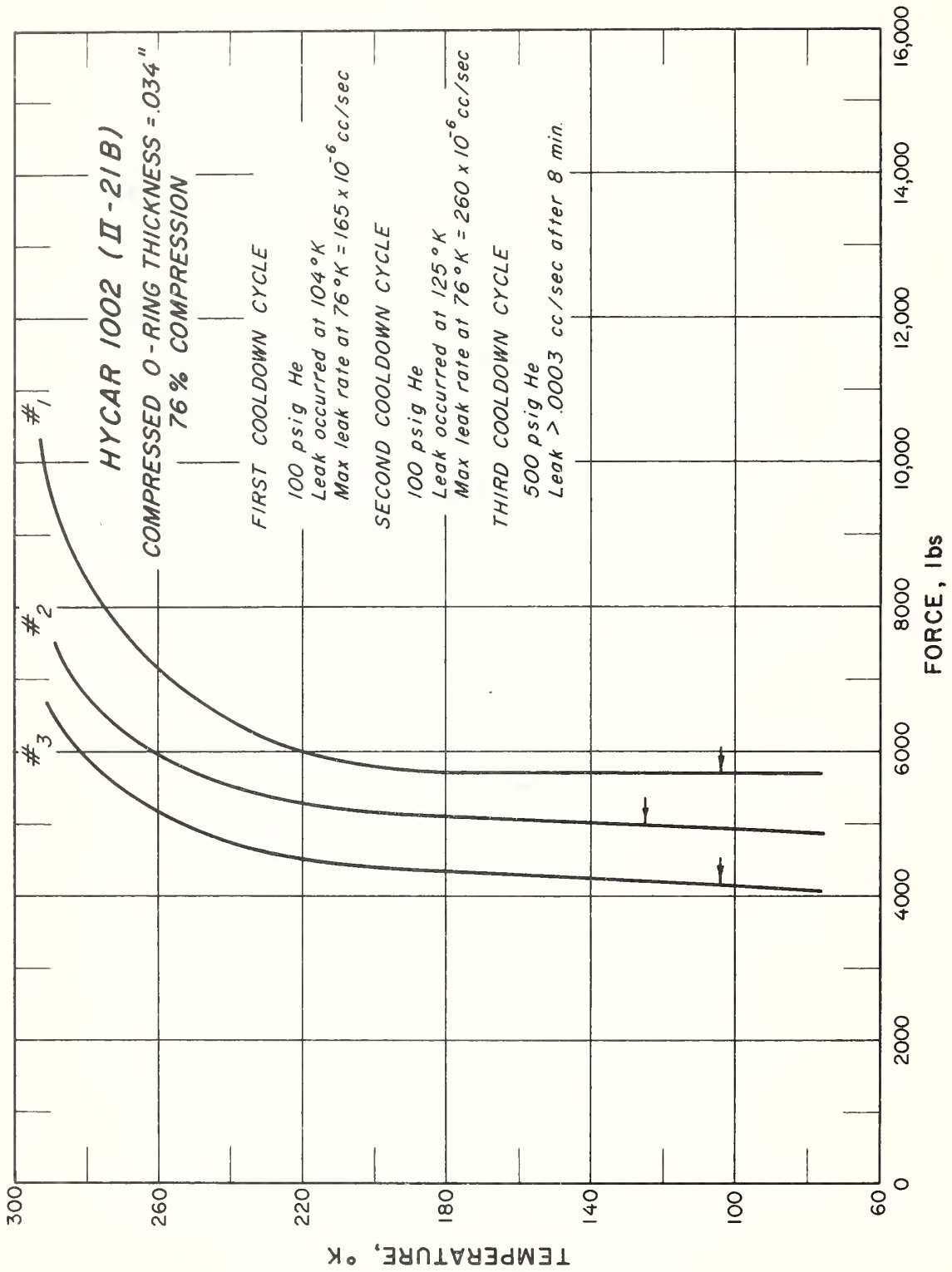


Figure 10. Force-Temperature Curve, "Hycar" 1002

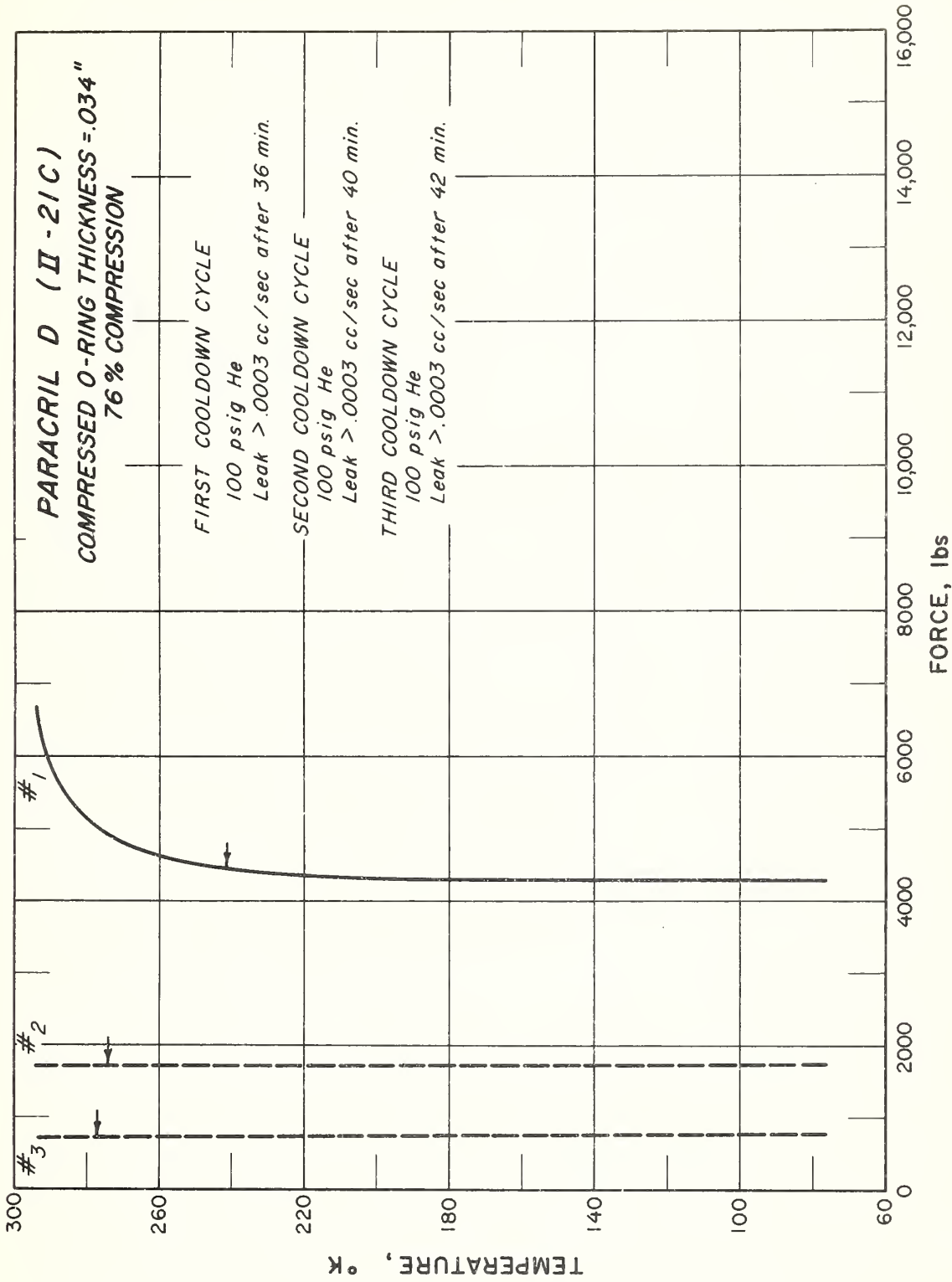


Figure 11. Force-Temperature Curve, "Paracril" D

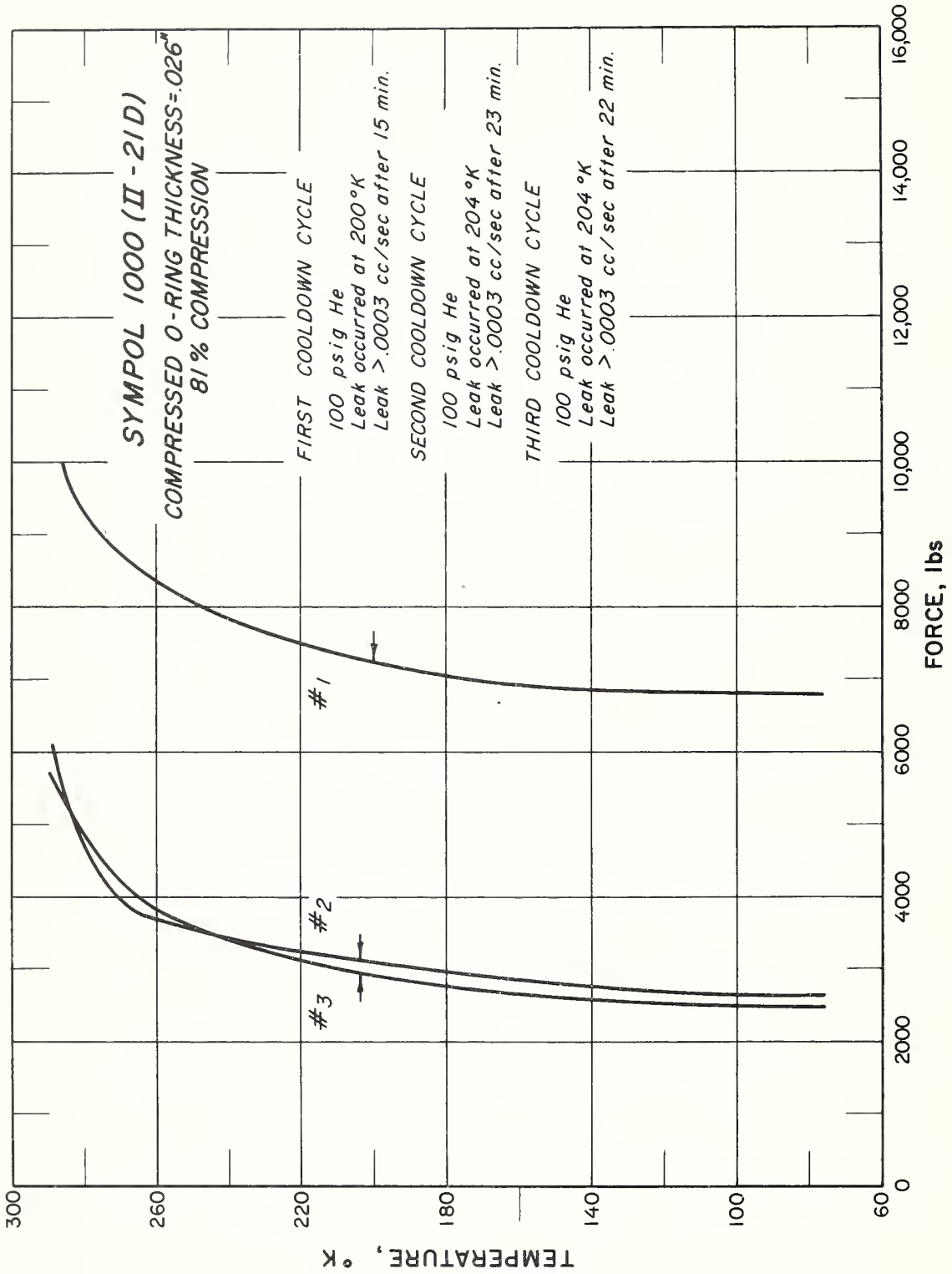


Figure 12. Force-Temperature Curve, "Sympol" 1000

performed better than any of the butadiene-acrylonitrile polymers. Only 27% of the initial force was lost before cooldown and the O-ring maintained 7500 pounds of force after the first cooldown. The O-ring began leaking at 104°K during the first cooldown. After being cooled to 76°K, the leak rate was constant at 165×10^{-6} atm cc/sec. The second cooldown pressure was also 100 psig helium. The leak rate at 76°K was 260×10^{-6} atm cc/sec. The helium pressure was increased to 500 psig for the third cooldown. The O-ring began to leak at 104°K and the leak rate exceeded 0.0003 atm cc/sec. before the O-ring temperature reached 76°K. The compression set was also very low (32%).

The above three polymers of butadiene-acrylonitrile all have the same compounding recipe and cure treatment. This leads one to conclude that 70/30 is near the optimum monomer ratio for good seal performance of these copolymers.

Most of the polymers in group IV performed comparatively well. Four different ethylene-propylene (IV-29C) O-rings were compressed in an effort to build up 14,000 pounds of force and keep the O-ring confined between the compression disc and base. This compound has a peculiar characteristic, in that one segment of the O-ring always extrudes out from under the compression disc. It was impossible to keep all of the O-ring under the compression disc. Force-temperature curves, figure 13, were obtained for this compound but the leak test is not valid because of the O-ring extrusion. The O-ring maintained 9,000 pounds of the initial force after the first cooldown and would probably maintain a seal to a much lower temperature if a harder compound near 80 durometer could be obtained. This would help eliminate the extrusion problem.

Cis-4 Polybutadiene (IV-29B), figure 14, performed the best of all the elastomer samples tested at 14,000 pounds initial force. Only 29% of the initial force was lost before cooldown and 8,000 pounds of force was maintained after the first cooldown cycle. The compression set was only 23%. No leak occurred during the first cooldown cycle at 100 psig helium pressure. For the second cooldown cycle at 500 psig pressure, no leak occurred. A leak did occur during the third cooldown cycle at a temperature of 123°K and 1,000 psig pressure.

When the leak occurred, the force had decayed to approximately 500 pounds. Since the gas pressure on the compression disc inside the compressed O-ring would account for most of this force, it

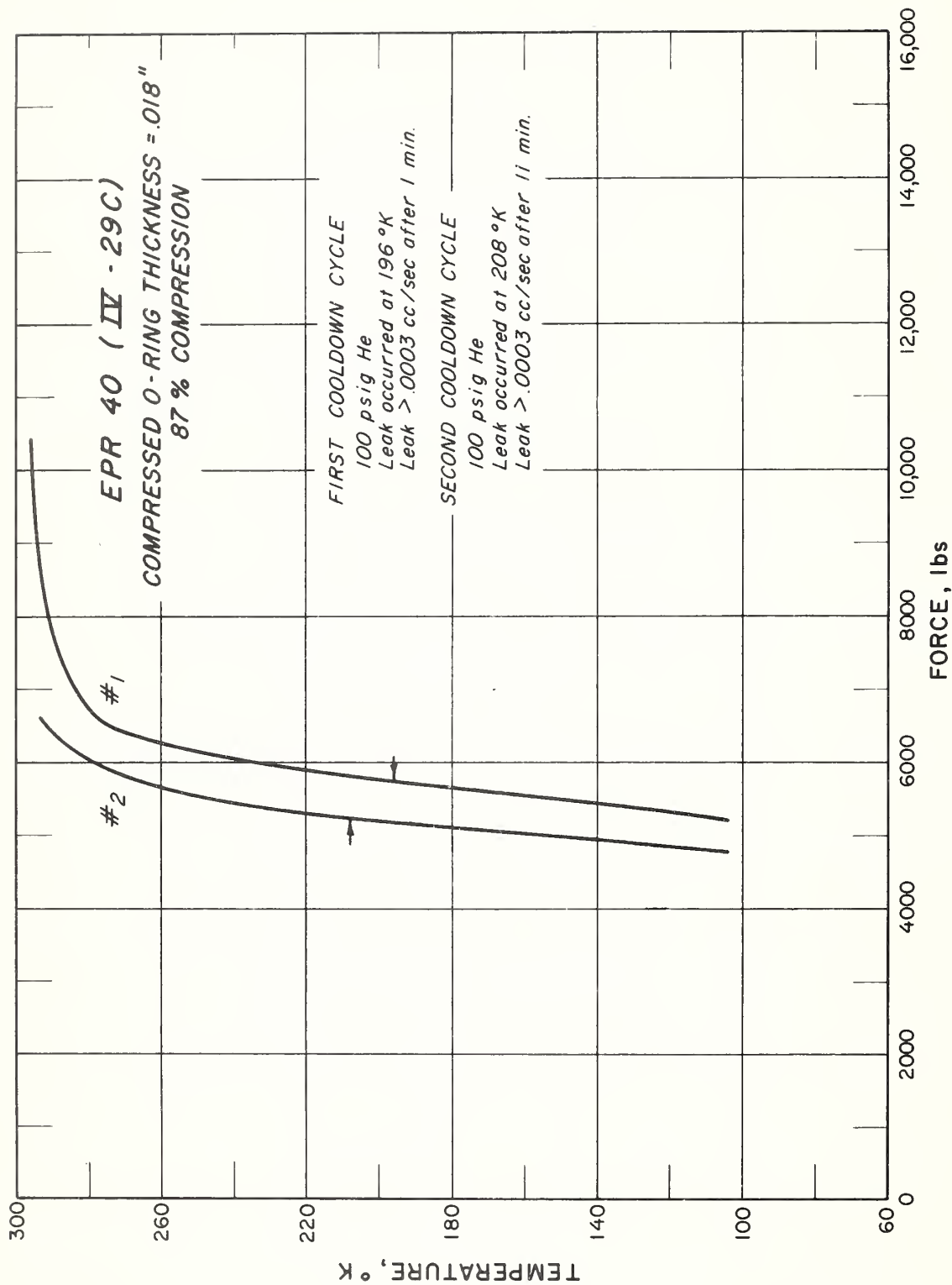


Figure 13. Force-Temperature Curve, Ethylene Propylene Rubber

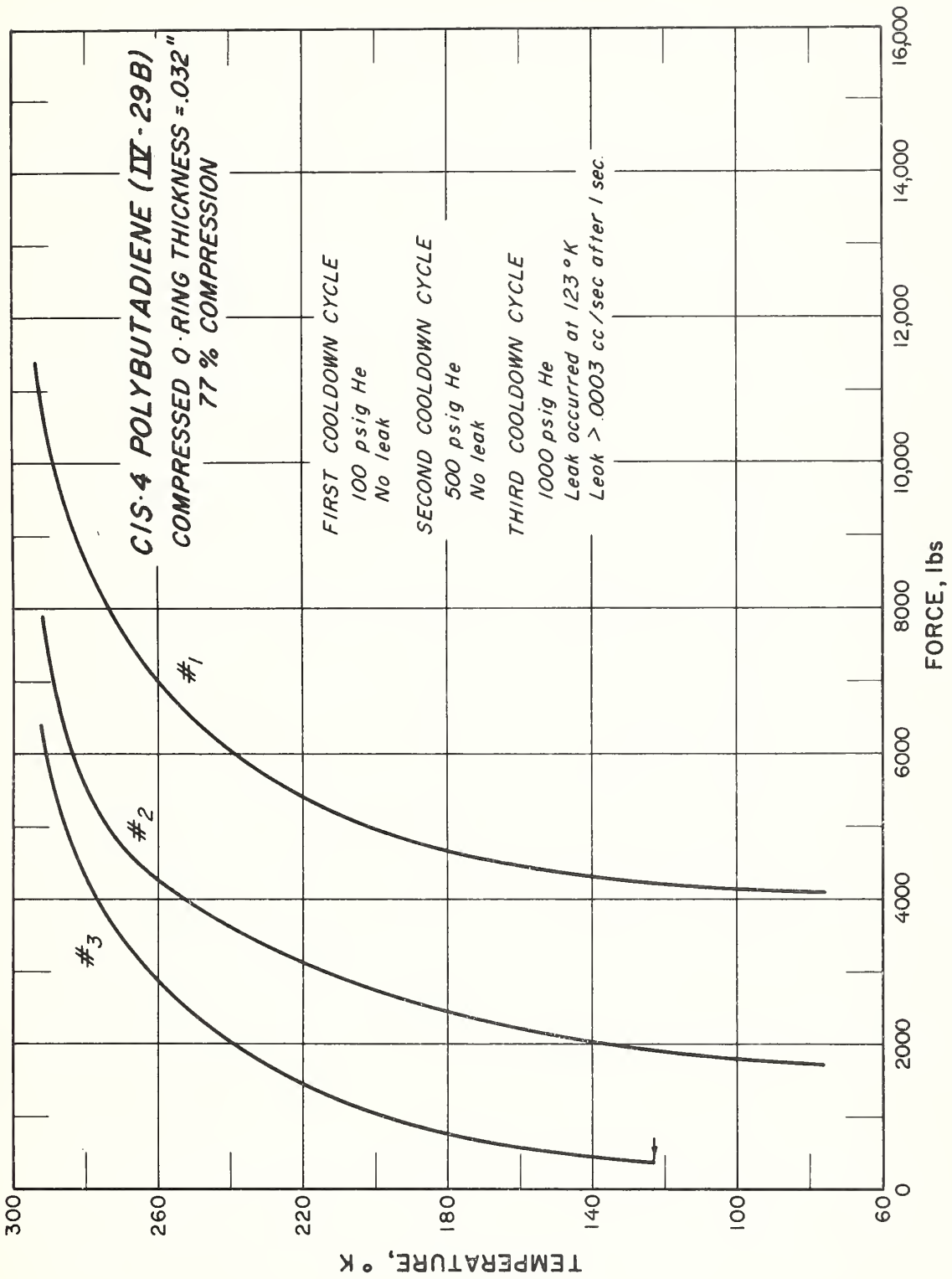


Figure 14. Force-Temperature Curve, Polybutadiene

appears that the compression force on the O-ring when it leaked was almost zero. One might expect this to always be the case, but most of the O-rings begin to leak while the compression force on the O-ring is still quite high. It appears likely that small leak passages can occur with some of the elastomers even though most of the sealing surface is under high compressive force. This may indicate some irregularity or nonuniformity in the way highly compressed materials contract when they are cooled.

Cis-4 polybutadiene has still another virtue. From recent tests in thermal expansion, it has been determined that T_g for this compound is approximately 168°K. T_g for most of the other elastomer samples extends from 202°K to 262°K. This lower brittle point temperature may well be a contributing factor to its excellent seal performance.

Two separate tests were made using A. S. D. natural rubber (IV-8A), one with 14,000 pounds initial force, figure 15, and the other with 18,000 pounds initial force, figure 16. The O-ring that was given 14,000 pounds initial force lost only 17% before cooldown. After the first cooldown cycle the O-ring still maintained a force of 9200 pounds. This compound loses very little force. However, in spite of the high force maintained by the O-ring, the seal leaked at 154°K during the first cooldown, and at 169°K for the second and third cooldown cycles.

The O-ring that was given 18,000 pounds initial force lost only 27% before cooldown. After the first cooldown cycle the O-ring still maintained a force of 12,000 pounds. No leak occurred during the cooldown cycles at 100, 500, and 1,000 psig respectively. However, when the test jig was removed from the dewar and jarred on the concrete floor, a leak occurred at 76°K and 1250 psig helium pressure. The O-ring compression was 83% and there was no material failure. Results from this and previous tests indicate that natural rubber will make a reliable seal at 76°K if given an adequate amount of compression (83-90%).

Polyisoprene (IV-29A) figure 17, lost only 18% of the initial force before cooldown and the O-ring maintained a force of 7200 pounds after the first cooldown. A small leak occurred at 88°K during the first cooldown with 100 psig helium pressure. At 76°K the leak rate had increased to and become constant at 8×10^{-6} atm cc/sec. The helium pressure inside the O-ring was increased to

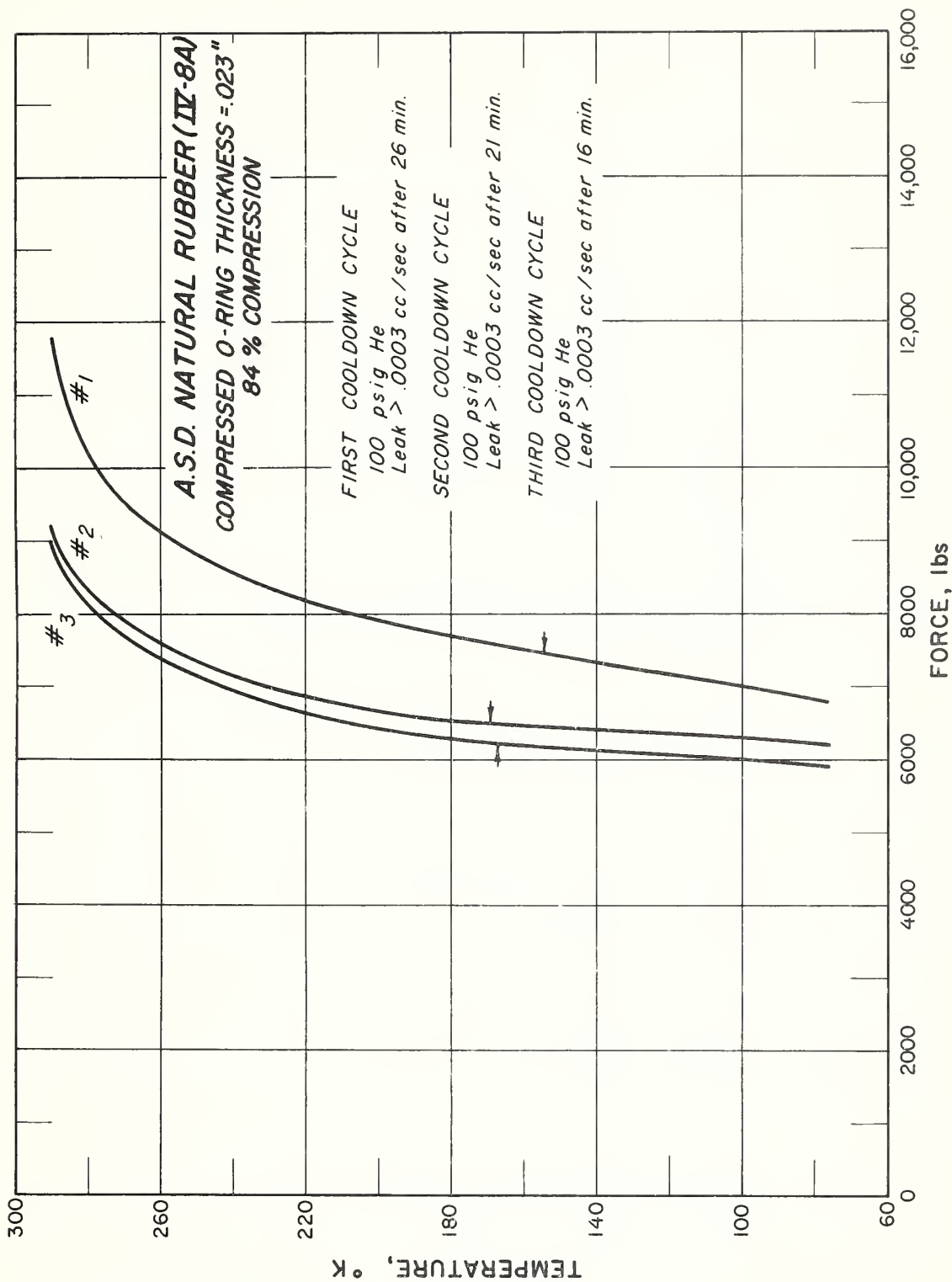


Figure 15. Force-Temperature Curve, Natural Rubber

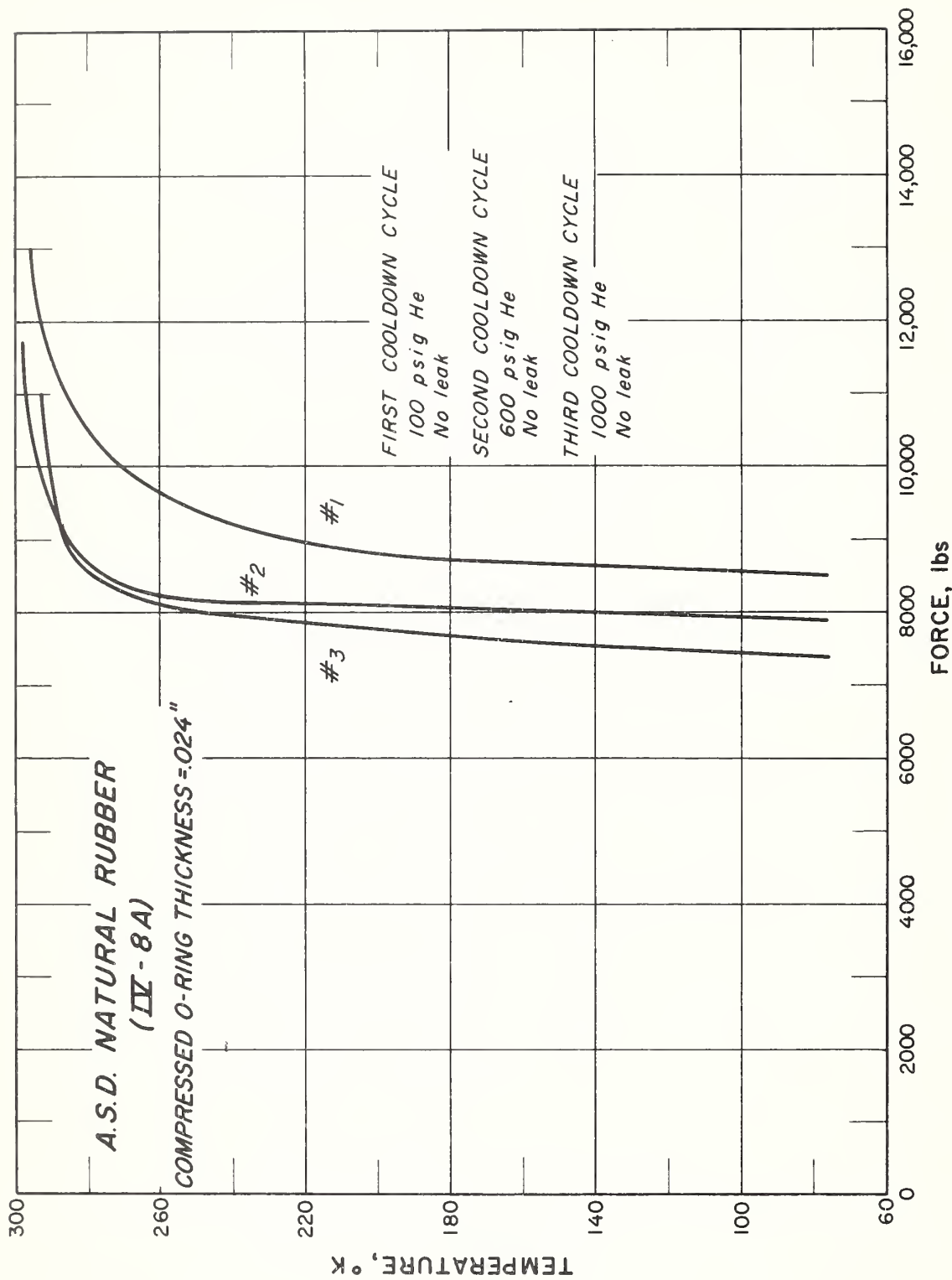


Figure 16. Force-Temperature Curve, Natural Rubber

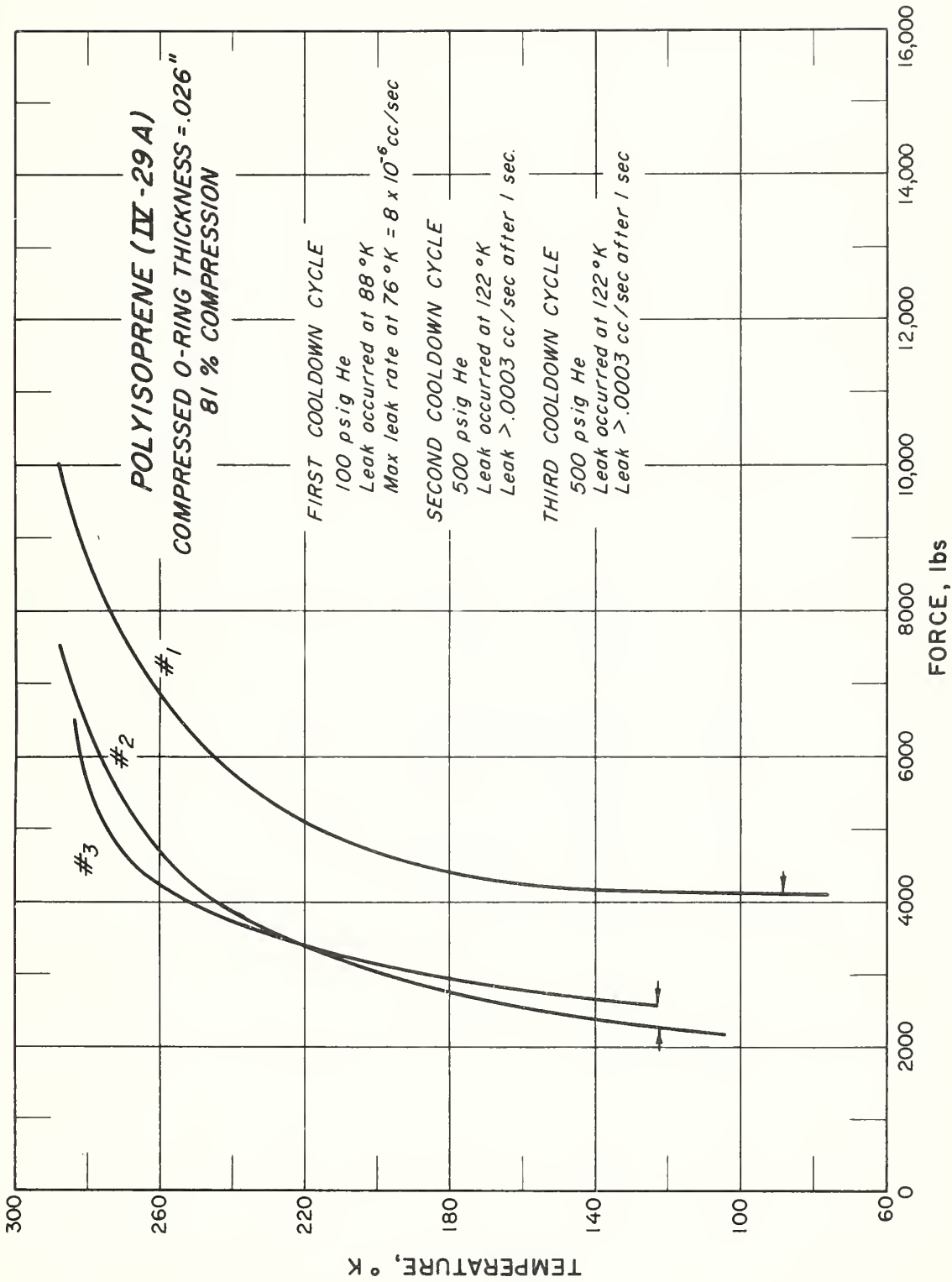


Figure 17. Force-Temperature Curve, Polyisoprene

500 psig for the second and third cooldown. A leak began at 122°K for each cycle and exceeded 0.0003 atm cc/sec. immediately. Examination of the O-ring after testing revealed small pock marks or pits in the compressed surfaces of the O-ring. This pitting was not observed in the other elastomer samples of this group and may be due to the milling procedure.

Neoprene (IV-8B), figure 18, lost 48% of its initial force before cooldown. This compound maintained less of the initial force than the other compounds of this group. The compression set was also high (85%). However, in previous tests, "Neoprene" has made excellent seals at slightly higher compression.

The compounds in group IV showed the least force decay and have good sealing ability. It is felt that all of the elastomer samples in group IV, except the present compound of ethylene-propylene rubber, would maintain a good seal at 76°K if given an initial force of 18,000 pounds.

1.4 Conclusions

Several observations have been made in the testing to date. If an O-ring leaks, there is very little difference in the leak temperature for the second and third cooldown, and the leak temperature is usually lower for the first cooldown cycle. The lower leak temperature for the first cycle is probably due to the higher force present at the start of the first cooldown. But, after the soldering procedure and one cooldown cycle, the O-rings tend to come to equilibrium and maintain a fairly constant force for the second and third cooldown cycles. Hence, the constant leak temperature for these last two cooldown cycles. There appears to be a strong correlation between the force on a given O-ring and the temperature at which it leaks.

Another observation during the testing is the relative unimportance of the cooldown pressure. It seems that if an O-ring will hold a seal at 76°K with 100 psig helium pressure, it has an excellent chance of maintaining this seal at 76°K and 500 psig helium pressure. There has been no test made to date where a seal leaked at 500 psig and not 100 psig. Also, most O-rings that hold 100 psig helium pressure at 76°K have a good chance of maintaining a seal at 1,000 psig pressure and 76°K, or at least to a temperature near 76°K.

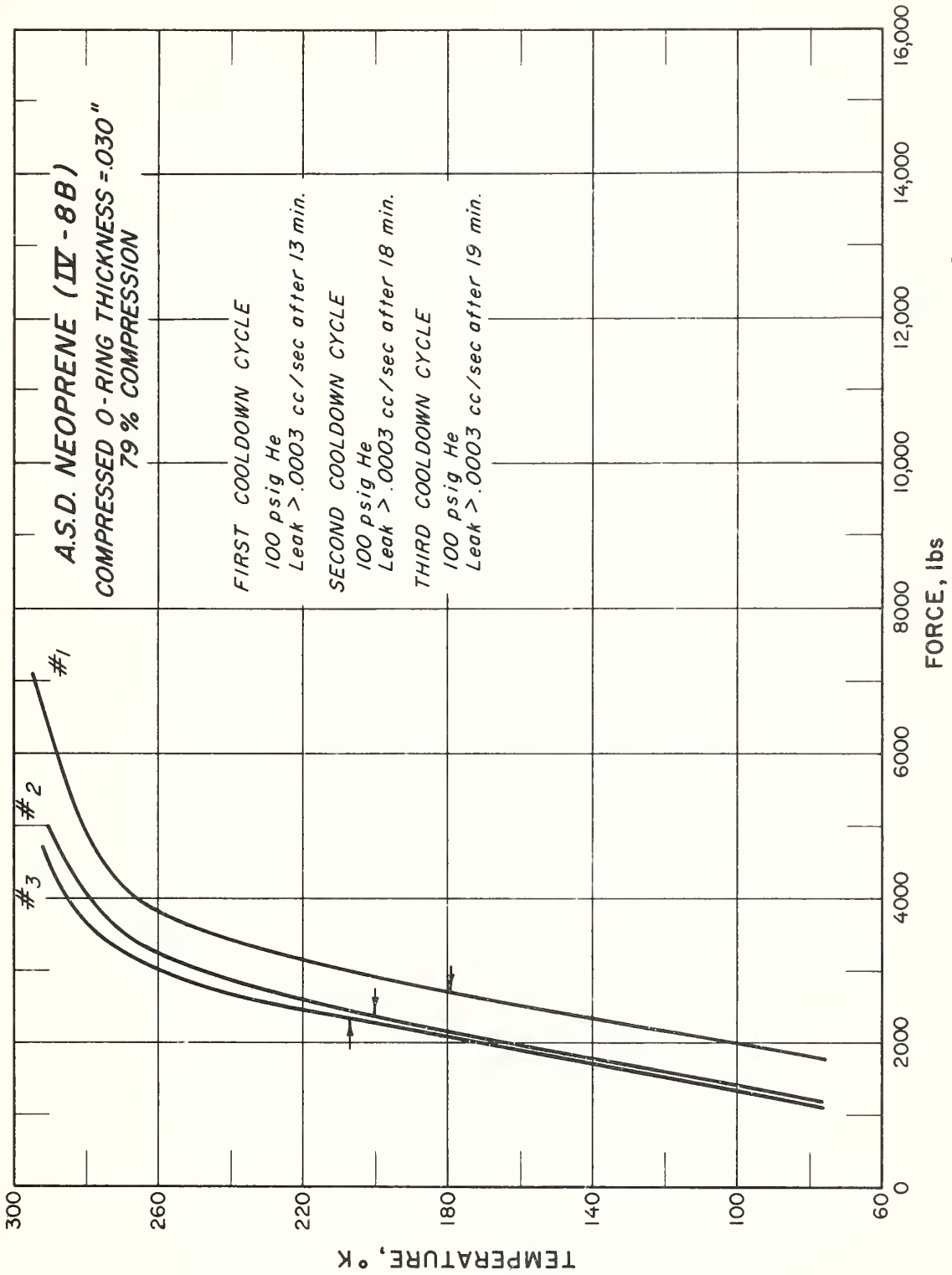


Figure 18 Force-Temperature Curve, "Neoprene"

Still another observation is the absence of any change in force at the point where the leak occurs. This further enforces the theory of small leak passages that may develop even though there is considerable compressive force on most of the sealing surface.

Another observation in all of these tests is the absence of any significant change in the force-temperature curves as the elastomer passes through the glassy state transition temperature (T_g). Possibly the high compression, close confinement due to friction, and low final thickness combine to prevent the material from showing any sudden change as it passes through the transition temperature.

Force-temperature curves for additional A. S. D. materials will be presented and compared in subsequent reports.

2.0 Thermal Expansion (Y. O.)

2.1 Introduction

During this reporting period group II, consisting of butadiene/styrene and butadiene/acrylonitrile copolymers, was completed. The results are given in Figure 19 and Table 3, and examined in the following paragraphs.

2.2 Results

Samples in group II consist of two sub-groups. One consists of butadiene/styrene polymers; the other butadiene/acrylonitrile.

The butadiene/styrene samples, "Synpol" 1000 and "Synpol" 1013, differ only by their monomer ratios, 77/23, 57/43, respectively. "Synpol" 1013, having a larger proportion of styrene than "Synpol" 1000, has a higher T_g and a smaller $\Delta L/L$. The unfilled sample of "Synpol" 1000 gives a T_g which is equal to that of the filled sample. In this case, it seems that carbon black does not affect the T_g but does influence the $\Delta L/L$, lowering it some 17%.

The butadiene/acrylonitrile polymers, "Paracril" 18/80, "Hycar" 1002 and "Paracril" D, have monomer ratios, 80/18, 70/30, and 45/55, respectively. Since acrylonitrile is highly polar, one would expect an increasing order of T_g , which so results. There were two samples of "Paracril" 18/80, filled and unfilled. The filled sample had a higher T_g by $9K^\circ$.

Comparing results for "Synpol" 1000 [butadiene/styrene, 77/23] with "Paracril" 18/80 [butadiene/acrylonitrile, 80/18], we see that "Synpol" 1000 has a T_g $18K^\circ$ lower than that of "Paracril" 18/80. Comparing the corresponding unfilled samples, we observe a difference of $9K^\circ$.

"Synpol" 1000 filled with 31.3% carbon black has a $\Delta L/L$ of 0.0215; "Paracril" 18/80 filled with 26.6% carbon black has a $\Delta L/L$ of 0.0209, a slight difference of 2.8%.

The unfilled corresponding samples have similar compounding recipes, except for the gum. The only difference otherwise is that "Synpol" 1000 has 2 parts sulfur, while "Paracril" 18/80 has 1.5 parts.

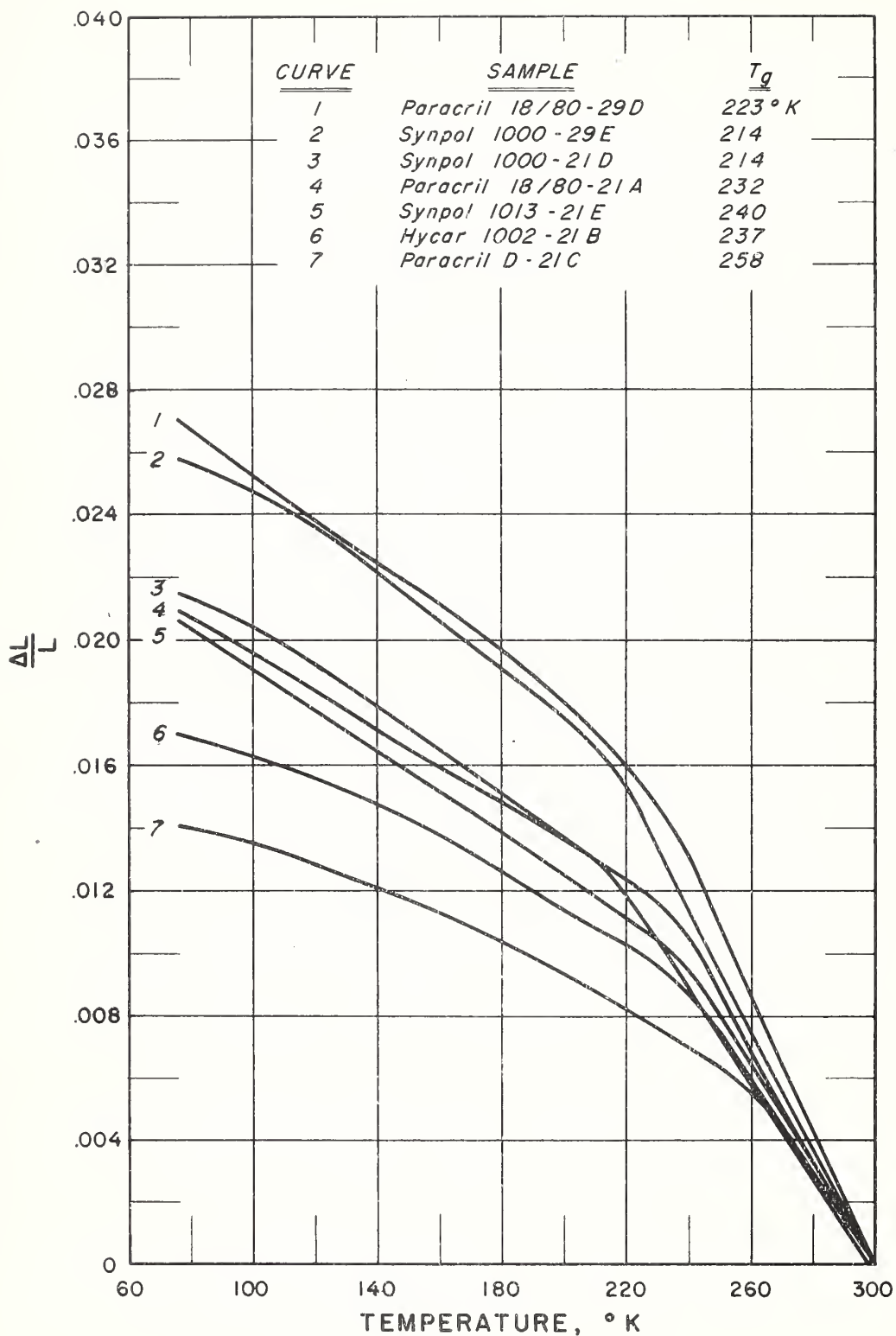


Figure 19. Linear Thermal Expansion and T_g , Group II [

33
Table 3

Summary of Thermal Expansion and T_g Results, Group II

Sample	T_g ($^{\circ}\text{K}$)		Experi- mental	α_r ($^{\circ}\text{K}^{-1}$)	α_g ($^{\circ}\text{K}^{-1}$)	*a_2 ($^{\circ}\text{K}^{-1}$)	$\Delta L/L$ from 297 $^{\circ}\text{K}$ to 76 $^{\circ}\text{K}$
	Theoretical						
	*Eq. (7)	*Eq. (6)					
"Synpol" 1000-21D	213	212	214	1.5×10^{-4}	$.68 \times 10^{-4}$	2.4×10^{-4}	2.15×10^{-2}
"Synpol" 1000-29E	213	212	214	2.0	.76	3.6	2.59
"Synpol" 1013-21E	240	239	240	1.6	.69	2.7	2.05
"Paracril" 18/80-21A			232	1.8	.58	3.6	2.09
"Paracril" 18/18-29D			223	2.2	.72	4.5	2.70
"Hycar" 1002-21B			237	1.5	.56	2.7	1.71
"Paracril" D-21C			258	1.5	.56	2.7	1.41

*Eq. (6)^[1]:

$$\frac{1}{T_g} = \frac{W_1}{T_{g1}} + \frac{W_2}{T_{g2}}$$

T_{g1} and T_{g2} apply to the homopolymers; W_1 and W_2 their respective weight fractions.

Eq. (7):

$$T_g = X_1 T_{g1} + X_2 T_{g2}$$

X_1 and X_2 are the mole fractions of the homopolymers.

*a_2 [1] = $\alpha_r - \alpha_g$, where α_r = the volume expansion coefficient in the rubbery state and α_g = that in glassy state.

The $\Delta L/L$ of unfilled "Synpol" 1000 is 0.0259; that of unfilled "Paracril" 18/80 is 0.0270.

From the above comparisons one may conclude that the acrylonitrile affects the T_g of the copolymer much more than does the styrene. But that styrene influences the $\Delta L/L$ as much as, if not more, than acrylonitrile does. Styrene is stiff and offers steric hinderance. That is, the large phenyl group protrudes and prevents easy movements, besides being cumbersome. This stiffness contributes to the lowering of the T_g in a copolymer, but acrylonitrile with its very strong polar points presents a more formidable barrier for rotation and hence has a more pronounced effect. It is possible to explain the effect of styrene on $\Delta L/L$ by dwelling again on the protruding phenyl groups. They serve as "hooks" to entrap the molecular chains so that it is difficult for them to move past each other. These "hooks" seem to be more effective in this type of restriction than the short range polar forces of acrylonitrile.

3.0 Volume Compression and the Glassy State Transition. (R. F. R.)

3.1 Introduction

When an elastomer is subjected to high unidirectional compression, as in the case of O-rings for low temperature service, a certain amount of volume compression results from retaining forces in the elastomer and frictional forces at the bearing faces. The speculation arose that this volume compression could change the temperature at which an elastomer becomes hard and glassy, since the free volume for chain movement is reduced. The change in this temperature (T_g) would, of course, affect overall thermal expansion or contraction, force decay curves, and possibly O-ring sealability at low temperatures. Hence a small program to investigate the effects of volume compression on T_g has been initiated.

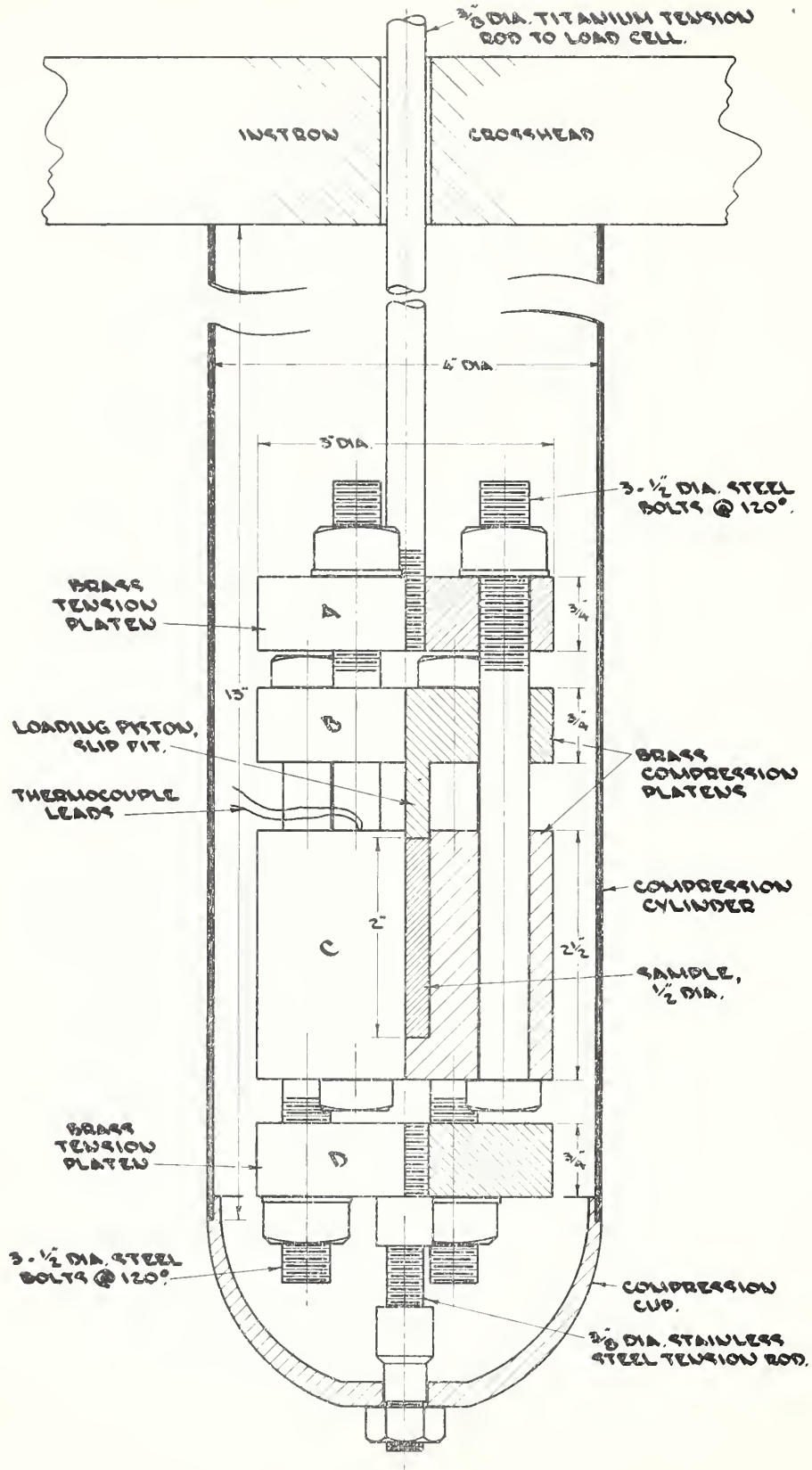
The tests are not connected with analysis of force decay, except as a means to an end. It has been previously observed [2, 3] that if an applied force is measured during a temperature change, the sample being maintained at constant length, a change in slope occurs at T_g sufficient to determine T_g from the force measurement. Using this device for determining T_g we propose to find a relation between T_g and volume compression for various elastomers.

3.2 Apparatus and Procedure

The Instron tensile testing machine of section 81.30 NBS was chosen for the constant length process since the moving crosshead is easily kept stationary. Figure 20 shows the volume compression jig as it is placed on the Instron. A tensile load is applied to the tension platens by moving the crosshead downward. As the crosshead moves downward, the stainless steel compression cylinder and the compression cup move the lower brass tension platen "D". This in turn moves the upper brass compression platen "B" downward, compressing the sample. The load is measured through a titanium pull rod by a load cell, which is in the upper stationary crosshead of the Instron. Parts "A" and "C" remain stationary during the loading period.

The sample area was designed to accommodate 2 inch x 1/2 inch diameter samples supplied by ASD for the thermal expansion program. The samples fit snugly in the sample area, and it is assumed that all linear movement of the upper compression platen (after it is in place) imparts volume compression to the sample. The piston of the platen fits snugly into the sample cavity, assuring no extrusion of sample material during compression. A thermocouple located near the sample measures a temperature believed to be within a few degrees of the actual temperature of the elastomer; however, the magnitude of error introduced here is unknown.

The test procedure is as follows: An elastomeric sample is inserted in the jig, and a dewar is secured around the test area by suspension from the moving crosshead. The sample is compressed by moving the crosshead. Deflection of the loading members is estimated from Young's modulus, and is subtracted from crosshead travel to determine changes in length of the sample. Initial volume compression can be determined from length changes of the sample, since the sample cross-sectional area remains constant. Cooling is then initiated by pressurizing the ullage volume over a 50 liter liquid nitrogen dewar, and force is monitored during cooldown. The compression cylinder and cup cool rapidly, causing immediate unloading of the sample. The reduction in compression due to this unloading is subtracted from the compression before cooling to arrive at an approximate percent compression just before the sample becomes brittle. When the sample temperature is well below T_g , the dewar is removed and force is monitored while the sample warms to a temperature well above T_g . Force data is automatically



D-5201

FIGURE 20 - VOLUME COMPRESSION APPARATUS

recorded continuously, and thermocouple data is manually taken periodically.

3.3 Typical Force and Temperature Histories

To date four tests have been performed, the data taking the shape found in figure 21, which is test I-5, natural rubber. The solid line represents force history, the dotted line temperature history as represented by the copper-constantan thermocouple potential. At 300°K , $\Delta E = 0$, $\Delta E = 6.6$ at 76°K . The sample is loaded well before time zero and allowed to relax until no appreciable force change is taking place. As cooling begins (time zero) rapid force decay is caused by three distinct mechanisms: 1) The characteristic volume contraction of the material; 2) The linear contraction of the compression cylinder; 3) The Gouge-Joule effect, which has been described previously [4]. Since the compression cylinder cools quite rapidly, only the other effects and smaller dimension changes in the jig are present after 20 minutes of cooling. At T_g the apparent volume contraction is reduced and the Gouge-Joule effect ceases to exist, and the force decay levels off.

In the test of figure 21 the dewar is removed after 50 minutes. Heat from the surroundings immediately warms the compression cylinder causing a rapid force increase which levels off after about ten minutes. As warming progresses the force continues to increase slowly until the transition region is reached. As the material "softens" the force decays, and then recovers, after which force increases at a higher rate than below T_g .

From this figure it can be seen that no clear cut evaluation of force decay data can be made, since length changes in the compression cylinder cause large force changes independent of the elastomer. However, the test is not designed to quantitatively measure force decay; it merely uses force changes to observe T_g under the conditions of volume compression. It is obvious that T_g can be readily observed, and future test results will help clarify the shapes of the curves under different cooling conditions. However, the test results available at present have yielded some interesting and possibly important information, which will be discussed in the next sections.

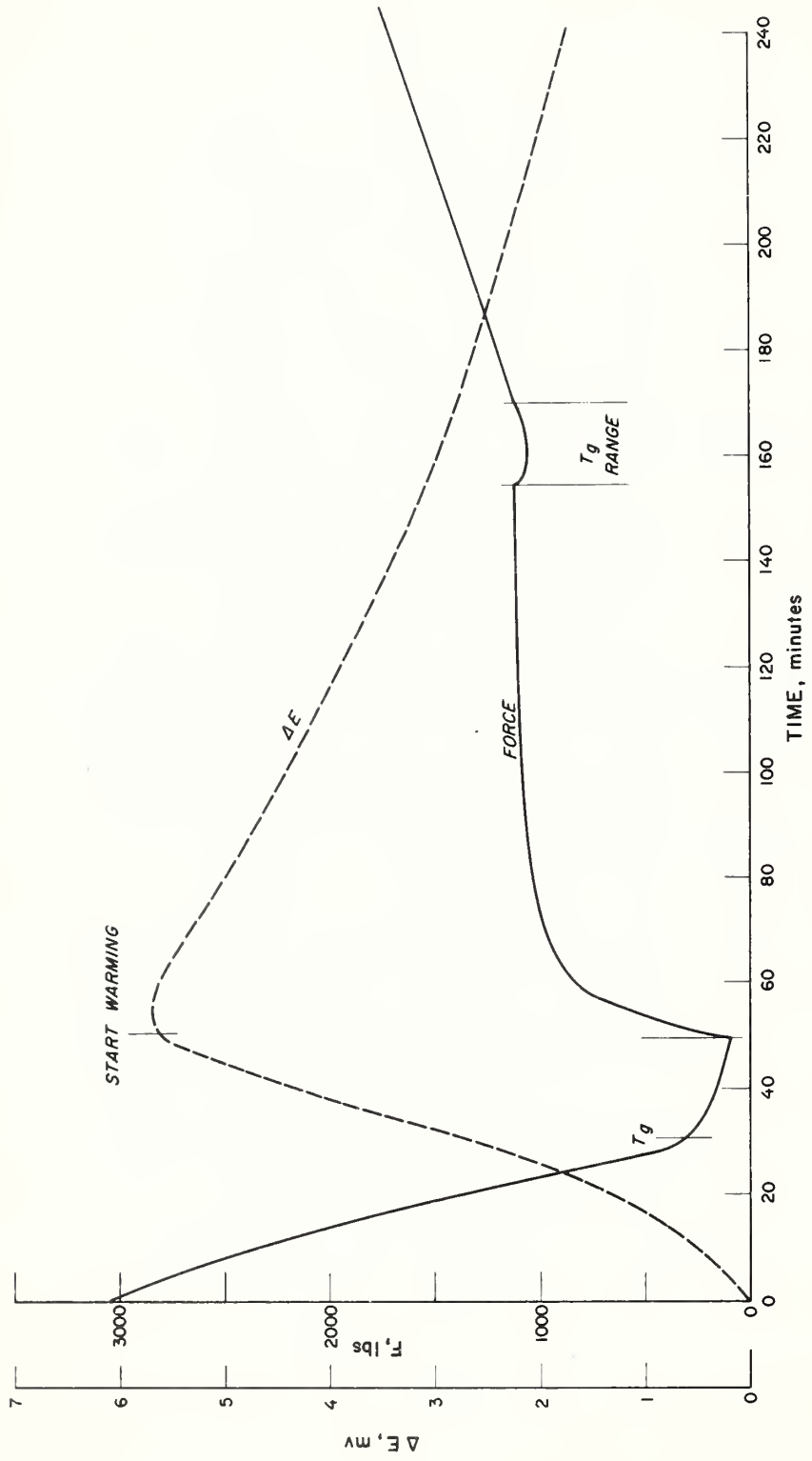


Figure 21. Volume Compression - Typical Force and Temperature Histories, NBS Natural

3.4 The Glassy State Transition

In figure 22 the data in figure 21 are cross plotted to obtain Force versus Thermocouple Potential (ΔE) in the region of the glassy state transition. In order to better compare the cooling and warming portions, the curves are shifted so that T_g appears to be in the same force region for both curves. It is most interesting to speculate on the differences in shape of the warming curve and the cooling curve as they pass through the transition region. Whereas the cooling curve undergoes a gradual leveling at T_g , the warming curve takes a sharp dip resulting in a minimum somewhat similar to the minimum noted in resilience tests previously reported [1]. This minimum is intuitively expected; it seems quite natural that when a brittle material softens, the force will decay. However, theoretical force decay considerations do not predict such a minimum. A fairly general force decay equation which has previously been reported [4] predicts that a change in force due to a change in temperature (neglecting time effects) is a function only of the Young's moduli and coefficients of expansion of the sample and the loading members. Without regard to the shape of curve predicted by the theory, which is very hard to handle around T_g , it is apparent that the theory would predict identical curves for cooling and warming. It can be seen from figure 22 that this is not the case with our experimental results to date. The disagreement of the equation with the experimental will be examined further; possibly elimination of the compression cylinder would yield a different shape for the warming curve near T_g .

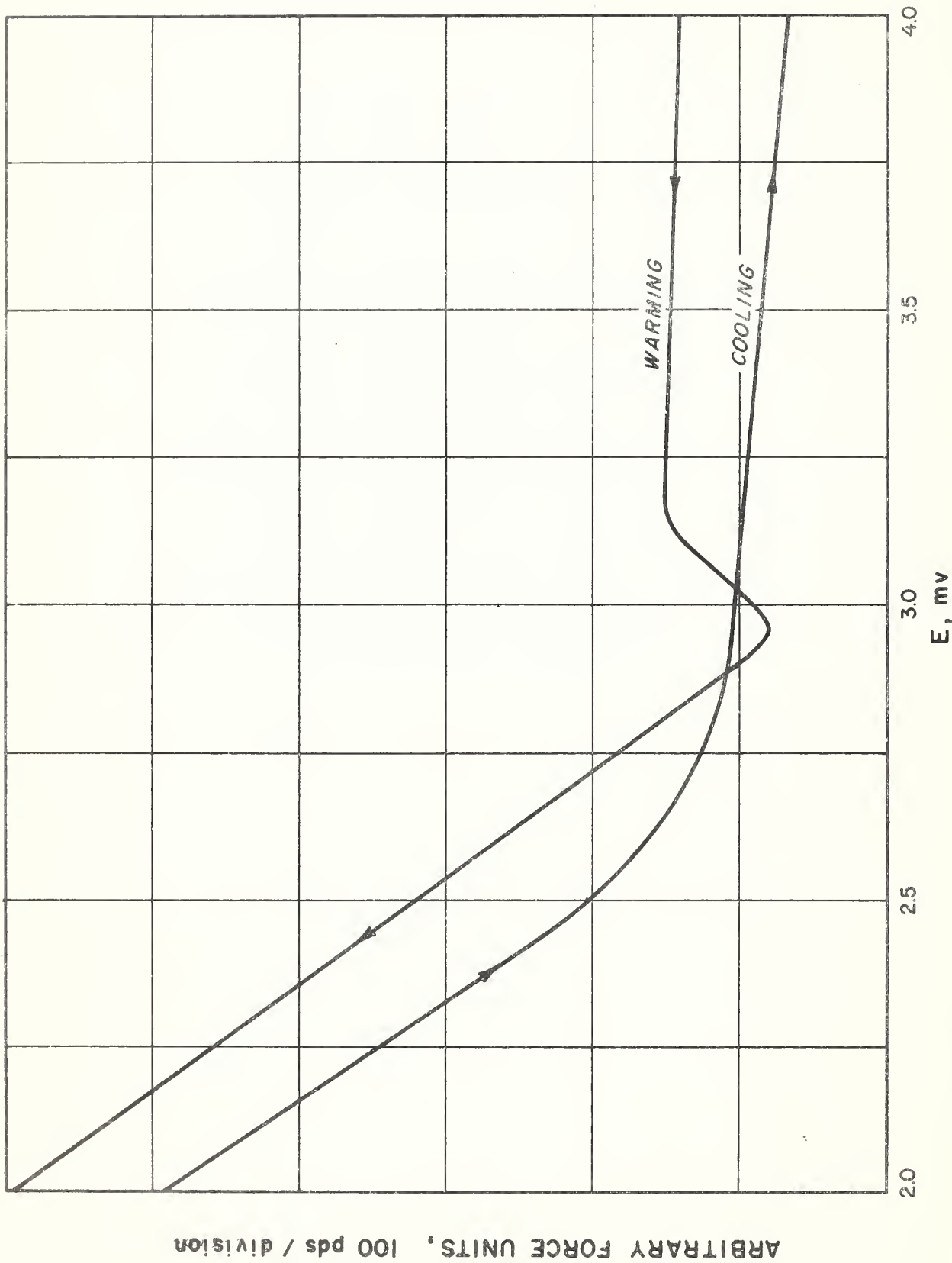


Figure 22. Force Changes in the T_g Range

3.5 A Relation Between T_g and Volume Compression.

Table 4 shows the experimental results to date. Three materials have been tested, tests I-3 and I-4 being run with different volume compressions on the same sample. Compounding recipes for the materials are shown in the appendix.

Table 4

Run	Material	Compound Number	T_{gf}^* (from force decay)	T_{ge} (from thermal expansion)	% change in T_g	% volume compression
I-2	Butyl 035		219	208	5.02	1.4
I-3	Silicone GE-555		188	157	16.80	4.0
I-4	Silicone GE-555		178	157	11.20	2.4
I-5	Natural Rubber		225	207	8.07	1.8

*Based on cooling curves only.

The last two columns in table 4 are plotted in figure 23 with percent volume compression on the logarithmic ordinate and percent change in T_g on the linear abscissa. When plotted in this way, the four data points available show a linear relation which is represented by the following equation:

$$\log_{10} (\% \text{ vol. comp.}) = 0.039 [\% \text{ change in } T_g] - 0.052$$

The equation is dimensionless, and represents the four experimental points to within 2%. This is rather phenomenal agreement, since it is not possible to determine T_g to 2% from force decay. Also, the estimates of volume compressions include educated guesses as to the effects of stretching of the loading members and contraction of the compression cylinder, and therefore could deviate by as much as 10-20% from the actual volume compression.

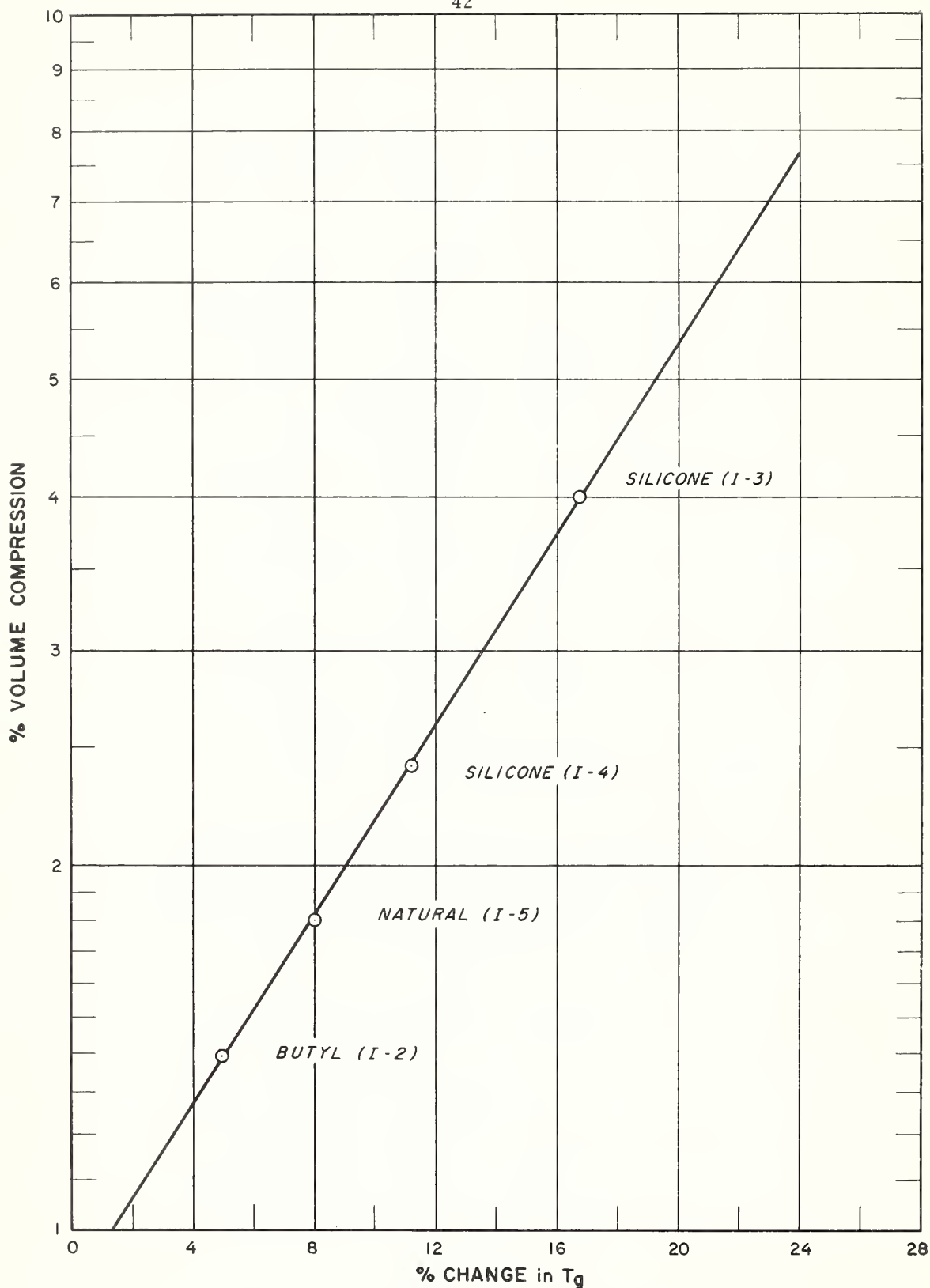


Figure 23. The Effect of Volume Compression on T_g

The good agreement is perhaps quite fortunate, but some correlation between volume compression and T_g for all materials was expected. It has been shown that the glassy state transition is a state of approximately constant fractional free volume for all high polymers [5]. Therefore all polymers should obey the same law regarding changes in T_g by volume compression, since the compression has a direct effect on the free volume available for chain rotation.

3.6 Summary

We have seen that volume compression has a direct effect on T_g . New values of T_g for compressed elastomers, as predicted by figure 23, could allow more careful theoretical analysis of the forces present in elastomeric O-ring seals. In future work, we will attempt to verify the results given here, and relate the behaviors to theoretical predictions.

References

1. Weitzel, D. H. , Robbins, R. F. , Ohori, Y. , and Ludtke, P. , Elastomeric Seals and Materials at Cryogenic Temperatures, NBS Report 7241, (April 1, 1962).
2. Weitzel, D. H. , Robbins, R. F. , Bopp, G. R. , Elastomers for Static Seals at Cryogenic Temperatures, Advances in Cryogenic Engineering VI (K. D. Timmerhaus, Editor), Plenum Press (1961).
3. Treloar, L. R. G. , The Physics of Rubber Elasticity, p. 26, Clarendon Press, Oxford, England (1958).
4. Robbins, R. F. , Weitzel, D. H. , and Herring, R. N. , The Application and Behavior of Elastomers at Cryogenic Temperatures, Advances in Cryogenic Engineering VII (K. D. Timmerhaus, Editor), Plenum Press (1962).
5. Tobolsky, A. V. , Properties and Structure of Polymers, p. 85, John Wiley and Sons, Inc. (1960).

Appendix. Compounding Recipes of ASD Materials

ASD No.	Polymer	Estimated Monomer Ratio	Recipe	Hardness (Shore A)	
<u>Group I</u>					
I-8D	Vinylidene Fluoride & Perfluoropropylene ("Viton" A, Du Pont)	70/30	Polymer Magnesium Oxide Hexamethylene Diamine Carbamate M T Carbon Black Cure 20 min at 280 F Post cure 16 hr at 400 F	100 20 1.3 25	80
I-12A	Vinylidene Fluoride & Perfluoropropylene (Third Monomer Unknown) ("Viton" B, Du Pont)	Terpolymer	Additives ditto 8D Cure 20 min at 310 F Post cure 16 hr at 400 F		75
I-12B	Vinylidene Fluoride & Perfluoropropylene ("Viton" A-HV, Du Pont)	70/30	Same as I-12A		80
I-12C	Vinylidene Fluoride & Perfluoropropylene ("Fluorel", Minnesota Mining & Mfg.)	70/30	Same as I-12A		80
I-12D	Vinylidene Fluoride & Monochlorotrifluoroethylene ("Kel F" 5500, Minnesota Mining & Mfg.)	50/50	Polymer Zinc Oxide "Hi Sil" Dibasic Lead Phosphite Benzoyl Peroxide Cure 20 min at 280 F Post cure 16 hr at 300 F	100 5 15 5 3	75
I-12E	Vinylidene Fluoride & Monochlorotrifluoroethylene ("Kel F" 3700, Minnesota Mining & Mfg.)	70/30	Polymer Zinc Oxide E P Carbon Black Dibasic Lead Phosphite Hexamethylene Diamine Carbamate Cure 30 min at 310 F Post cure 13 hr at 300 F	100 5 10 5 1.3	80

ASD No.	Polymer	Estimated Monomer Ratio	Recipe	Hardness (Shore A)
<u>Group II</u>				
II-21A	Butadiene & Acrylonitrile (¹¹ Paracril ¹¹ 18-80, Naugatuck Chem. Co.)	80/18	Polymer Zinc Oxide Altax (MBTS) Stearic Acid Sulfur FEF Black Cure 20 min at 310 F	100 5 1.5 1.5 1.5 50 75
II-21B	Butadiene & Acrylonitrile (¹¹ Hycar ¹¹ 1002, B. F. Goodrich Chem. Co.)	70/30	Same as II-21A	75
II-21C	Butadiene & Acrylonitrile (¹¹ Paracril ¹¹ D, Naugatuck Chem. Co.)	45/55	Same as II-21A	85
II-21D	Butadiene & Styrene (¹¹ S ynpol ¹¹ 1000, Texas-U. S. Chem. Co.)	77/23	Polymer Zinc Oxide Altax (MBTS) Stearic Acid Sulfur EPC Black Cure 50 min at 320 F	100 5 1.75 1.5 2 40 65
II-21E	Butadiene & Styrene (¹¹ S ynpol ¹¹ 1013, Texas-U. S. Chem. Co.)	57/43	Same as II-21D	70
II-29D	Butadiene & Styrene (¹¹ Paracril ¹¹ 18/80, Naugatuck Chem. Co.)	80/18	Polymer Zinc Oxide Stearic Acid Sulfur Altax Cure 30 min at 310 F	100 5 1.75 1.5 1.5 40
II-29E	Butadiene & Styrene (¹¹ S ynpol ¹¹ 1000, Texas-U. S. Chem. Co.)	77/23	Same as II-29D	40

ASD No.	Polymer	Estimated Monomer Ratio	Recipe	Hardness (Shore A)
<u>Group III</u>				
III-18C	Isobutylene & Isoprene (Butyl 035)	99/1	Polymer Zinc Oxide Stearic Acid Altax (MBTS) TMTDS Sulfur HAF Black Cure 30 min at 310 F	100 70 5 1 0.5 1 2 50
<u>Group IV</u>				
IV-8A	Natural Rubber (Smoked Sheet)		Polymer Stearic Acid Zinc Oxide N-Cyclohexyl-2-Benzothiazole Sulfenamide Sulfur High Abrasive Furnace Black Polymerized trimethyldi-hydroquinoline (Resin D) Cure 15 min at 310 F	100 65 3 5 .6 2.75 50 1
IV-8B	Chloroprene ("Neoprene," Du Pont)		Polymer Stearic Acid Zinc Oxide Magnesium Oxide High Modulus Furnace Black Na 22 Cure 20 min at 310 F	100 85 5 5 4 50 .5
IV-29A	Polyisoprene (Coral)		Polymer Zinc Oxide Stearic Acid Sulfur Santocure HAF Black Cure 20 min at 310 F	100 5 3 2.5 0.5 60

ASD No.	Polymer	Estimated Monomer Ratio	Recipe	Hardness (Shore A)	
IV-29B	Cis 4 Polybutadiene		Polymer	100	70
			Zinc Oxide	5	
			Stearic Acid	.5	
			Sulfur	2.5	
			High Abrasive Furnace Black	50	
			Cure 30 min at 310 F		
			IV-29C	Ethylene and Propylene (EPR-40)	
Stearic Acid	1				
Sulfur	.8				
High Abrasive Furnace Black	50				
Dicumyl Peroxide	4				
Cure 20 min at 310 F					

U. S. DEPARTMENT OF COMMERCE

Luther H. Hodges, *Secretary*

NATIONAL BUREAU OF STANDARDS

A. V. Astin, *Director*



THE NATIONAL BUREAU OF STANDARDS

The scope of activities of the National Bureau of Standards at its major laboratories in Washington, D.C., and Boulder, Colorado, is suggested in the following listing of the divisions and sections engaged in technical work. In general, each section carries out specialized research, development, and engineering in the field indicated by its title. A brief description of the activities, and of the resultant publications, appears on the inside of the front cover.

WASHINGTON, D. C.

Electricity. Resistance and Reactance. Electrochemistry. Electrical Instruments. Magnetic Measurements. Dielectrics. High Voltage.

Metrology. Photometry and Colorimetry. Refractometry. Photographic Research. Length. Engineering Metrology. Mass and Scale. Volumetry and Densimetry.

Heat. Temperature Physics. Heat Measurements. Cryogenic Physics. Equation of State. Statistical Physics.

Radiation Physics. X-ray. Radioactivity. Radiation Theory. High Energy Radiation. Radiological Equipment. Nucleonic Instrumentation. Neutron Physics.

Analytical and Inorganic Chemistry. Pure Substances. Spectrochemistry. Solution Chemistry. Standard Reference Materials. Applied Analytical Research. Crystal Chemistry.

Mechanics. Sound. Pressure and Vacuum. Fluid Mechanics. Engineering Mechanics. Rheology. Combustion Controls.

Polymers. Macromolecules: Synthesis and Structure. Polymer Chemistry. Polymer Physics. Polymer Characterization. Polymer Evaluation and Testing. Applied Polymer Standards and Research. Dental Research.

Metallurgy. Engineering Metallurgy. Microscopy and Diffraction. Metal Reactions. Metal Physics. Electrolysis and Metal Deposition.

Inorganic Solids. Engineering Ceramics. Glass. Solid State Chemistry. Crystal Growth. Physical Properties. Crystallography.

Building Research. Structural Engineering. Fire Research. Mechanical Systems. Organic Building Materials. Codes and Safety Standards. Heat Transfer. Inorganic Building Materials. Metallic Building Materials.

Applied Mathematics. Numerical Analysis. Computation. Statistical Engineering. Mathematical Physics. Operations Research.

Data Processing Systems. Components and Techniques. Computer Technology. Measurements Automation. Engineering Applications. Systems Analysis.

Atomic Physics. Spectroscopy. Infrared Spectroscopy. Solid State Physics. Electron Physics. Atomic Physics.

Instrumentation. Engineering Electronics. Electron Devices. Electronic Instrumentation. Mechanical Instruments. Basic Instrumentation.

Physical Chemistry. Thermochemistry. Surface Chemistry. Organic Chemistry. Molecular Spectroscopy. Molecular Kinetics. Mass Spectrometry.

Office of Weights and Measures.

BOULDER, COLO.

Cryogenic Engineering Laboratory. Cryogenic Equipment. Cryogenic Processes. Properties of Materials. Cryogenic Technical Services.

CENTRAL RADIO PROPAGATION LABORATORY

Ionosphere Research and Propagation. Low Frequency and Very Low Frequency Research. Ionosphere Research. Prediction Services. Sun-Earth Relationships. Field Engineering. Radio Warning Services. Vertical Soundings Research.

Radio Propagation Engineering. Data Reduction Instrumentation. Radio Noise. Tropospheric Measurements. Tropospheric Analysis. Propagation-Terrain Effects. Radio-Meteorology. Lower Atmosphere Physics.

Radio Systems. Applied Electromagnetic Theory. High Frequency and Very High Frequency Research. Modulation Research. Antenna Research. Navigation Systems.

Upper Atmosphere and Space Physics. Upper Atmosphere and Plasma Physics. Ionosphere and Exosphere Scatter. Airglow and Aurora. Ionospheric Radio Astronomy.

RADIO STANDARDS LABORATORY

Radio Physics. Radio Broadcast Service. Radio and Microwave Materials. Atomic Frequency and Time-Interval Standards. Millimeter-Wave Research.

Circuit Standards. High Frequency Electrical Standards. Microwave Circuit Standards. Electronic Calibration Center.

Department of Commerce
National Bureau of Standards
Boulder Laboratories
Boulder, Colorado

Official Business



Postage and Fees Paid
U. S. Department of Commerce